

7-31-2018

## Modeling of the Veterinary Anesthetic Circuit

Corinne Vilorio Duplantis

*Louisiana State University and Agricultural and Mechanical College*

Follow this and additional works at: [https://digitalcommons.lsu.edu/gradschool\\_theses](https://digitalcommons.lsu.edu/gradschool_theses)



Part of the [Computer-Aided Engineering and Design Commons](#)

---

### Recommended Citation

Duplantis, Corinne Vilorio, "Modeling of the Veterinary Anesthetic Circuit" (2018). *LSU Master's Theses*. 4779.

[https://digitalcommons.lsu.edu/gradschool\\_theses/4779](https://digitalcommons.lsu.edu/gradschool_theses/4779)

This Thesis is brought to you for free and open access by the Graduate School at LSU Digital Commons. It has been accepted for inclusion in LSU Master's Theses by an authorized graduate school editor of LSU Digital Commons. For more information, please contact [gradetd@lsu.edu](mailto:gradetd@lsu.edu).

# MODELING OF THE VETERINARY ANESTHETIC CIRCUIT

A Thesis

Submitted to the Graduate Faculty of the  
Louisiana State University and  
Agricultural and Mechanical College  
in partial fulfillment of the  
requirements for the degree of  
Master of Science

in

The Department of Mechanical and Industrial Engineering

by  
Corinne Vilorio Duplantis  
B.S., Louisiana State University, 2017  
December 2018

## **Acknowledgements**

I would like to acknowledge my advisor, Marcio de Queiroz, committee members Warren Waggenpack and Paulo Waltrich, and LSU School of Veterinary Medicine contact, Anderson da Cunha, for the guidance provided on this project. The NSF I-Corps program at LSU was instrumental in bringing me in touch with the veterinarians that face this problem as well as providing funding for research. I would also like to thank the Louisiana Board of Regents for providing me with a fellowship, making this research possible.

## Table of Contents

Acknowledgements.....	ii
List of Tables.....	iv
List of Figures .....	v
Abstract.....	viii
Chapter 1. Introduction.....	1
1.1 Background.....	1
1.2 Safety Relief Valves.....	5
1.3 Existing Solutions.....	6
1.4 Relevant Patents.....	8
1.5 Modeling of Anesthetic Circuits.....	9
1.6 Simscape.....	13
1.7 Motivation.....	14
Chapter 2. Methodology.....	15
2.1 Experimental Methods.....	15
2.2 Simscape Fluids.....	18
2.3 Model Description.....	19
Chapter 3. Results and Discussion.....	24
Chapter 4. Conclusions.....	39
References.....	41
Vita.....	43

## List of Tables

1. Variables from Mešić et al Model.....	12
2. Summary of Experimental Measurement Parameters.....	15
3. Pressure Drop Across Circuit Components for Various Flow Rates.....	24
4. Adjusted R-square Values for Valve Pressure Drop Regressions.....	27
5. Steady-state Error of Model Components.....	34
6. Flow Rates and Corresponding Patient Weight at 25 cmH <sub>2</sub> O Maximum Pressure.....	38

## List of Figures

1.	Bain Circuit.....	2
2.	Basic Rebreathing Anesthesia Machine Schematic.....	3
3.	Rebreathing Anesthesia Machine Image.....	4
4.	Simplified Diagram of Direct-Spring Operated SRVs.....	5
5.	Existing Solutions. a) Pop-Off Occlusion Valve; b) Safety Pop-Off Valve; c) EMD Safety Valve; d) Reverse-PEEP Valve.....	7
6.	Closed Exhaust Discharge System.....	8
7.	Dual Valve.....	8
8.	Ventilation Valve.....	9
9.	Anesthetic Circuit System Model.....	10
10.	Mešić et al Complete Model of Respiratory System.....	11
11.	Block Diagram of Rebreathing Anesthesia Machine.....	13
12.	Hydraulic Cylinder.....	14
13.	Experimental Setup Schematic 1.....	16
14.	Experimental Setup Schematic 2.....	17
15.	Experimental Setup Schematic 3.....	17
16.	Experimental Setup for Pop-off Valve.....	17
17.	Simscape Model of Veterinary Anesthesia System.....	20
18.	EMD Valve Addition.....	20
19.	Solver Configuration Block.....	21
20.	Custom Hydraulic Fluid Block.....	21
21.	Clock Block.....	21

22.	Oxygen Flow Source Connection.....	21
23.	Gas-Charged Accumulator Block.....	22
24.	Pressure Relief Valve Block.....	22
25.	Pop-off Valve Connection.....	23
26.	Patient Subsystem.....	23
27.	Pressure Sensor Subsystem.....	23
28.	Leak Subsystem.....	23
29.	One-way valve Flow Characteristic.....	25
30.	CO <sub>2</sub> Absorber Pressure Drop.....	25
31.	Pressure Drop Across Pop-off Valve set to 0 degrees.....	25
32.	Pressure Drop Across Pop-off Valve set to 180 degrees.....	26
33.	Pressure Drop Across Pop-off Valve set to 360 degrees.....	26
34.	Pressure Drop Across Pop-off Valve set to 540 degrees.....	26
35.	Pressure Drop Across Pop-off Valve set to 720 degrees.....	26
36.	Pressure Drop Across EMD Valve.....	26
37.	Pressure Drop Across Reverse-PEEP Valve.....	26
38.	Reservoir Bag Test Model.....	28
39.	Experimental and Simulated Pressure Response of Reservoir Bag at Various Flow Rates.....	28
40.	Relief Valve Test Model.....	29
41.	Experimental and Simulated Pressure Response of Pop-off Valve at 0 degrees at Various Flow Rates.....	29
42.	Experimental and Simulated Pressure Response of Pop-off Valve at 180 degrees at Various Flow Rates.....	30

43.	Experimental and Simulated Pressure Response of Pop-off Valve at 360 degrees at Various Flow Rates.....	30
44.	Experimental and Simulated Pressure Response of Pop-off Valve at 540 degrees at Various Flow Rates.....	31
45.	Experimental and Simulated Pressure Response of Pop-off Valve at 720 degrees at Various Flow Rates.....	31
46.	Experimental and Simulated Pressure Response of EMD Valve at Various Flow Rates....	32
47.	Experimental and Simulated Pressure Response of Reverse-PEEP Valve at Various Flow Rates.....	32
48.	Pressure Response of Anesthesia System Model at Various Input Flow Rates, Pop-off Valve at 0 degrees.....	33
49.	Pressure Response of Anesthesia System Model at Various Input Flow Rates, Pop-off Valve at 180 degrees.....	35
50.	Pressure Response of Anesthesia System Model at Various Input Flow Rates, Pop-off Valve at 360 degrees.....	35
51.	Pressure Response of Anesthesia System Model With Patient at Various Input Flow Rates, Pop-off Valve at 0 degrees.....	36
52.	Pressure Response of Anesthesia System Model With Patient at Various Input Flow Rates, Pop-off Valve at 180 degrees.....	36
53.	Pressure Response of Anesthesia System Model With Patient at Various Input Flow Rates, Pop-off Valve at 360 degrees.....	37
54.	Maximum System Pressure, Pop-off Valve at 0 degrees.....	38
55.	Maximum System Pressure, Pop-off Valve at 180 degrees.....	38
56.	Maximum System Pressure, Pop-off Valve at 360 degrees.....	38



## **Abstract**

Anesthesia is used to sedate both humans and animals for surgery. In veterinary practice, breathing systems are often used to supply anesthetic gas to the patient. Occasionally, a large amount of pressure can build up in the breathing circuit. This high pressure, if unnoticed, can lead to fatal injury to the lungs of the veterinary patient. The maximum allowable pressure in the anesthetic circuit for small animals is 25 cmH<sub>2</sub>O or 2450 Pa. As such, it is necessary to monitor oxygen flow rate (ranging from 0.1-4 LPM), pressure, oxygen rate, anesthetic composition, among other variables during an operation. Currently, not all veterinary anesthesia machines are equipped with a reliable way of detecting and relieving gas when dangerous pressures are reached. This thesis aims to understand veterinary anesthesia circuits and pressure relief systems and to formulate a Simscape Fluids model with components representative of real anesthesia machine components. The model was used to simulate the response of two commercially-available safety devices, the EMD Valve and Reverse-PEEP Valve, attached to the anesthesia system under various operating conditions. It was found that the Reverse-PEEP Valve is more effective at preventing lung injury to veterinary patients.

## **Chapter 1. Introduction**

In this chapter, the safety risk of the veterinary anesthetic circuit is presented. To understand the problems associated with the anesthesia machine, the circuit must first be understood. The operating principles of safety relief valves are explored, as they are used to regulate pressure and can keep the circuit at a safe pressure. Current solutions are explored, as well as relevant patents for anesthesia systems. Models of the respiratory system and anesthesia machines are reviewed, and an overview of the Simscape modeling environment is provided. The motivation and goals of the thesis are then explained.

### **1.1 Background**

Most surgical procedures for animals and humans require sedation of the patient via an anesthesia machine. Veterinary anesthesia machines differ slightly from anesthetic breathing systems made for humans, but largely operate on the same principles. Two main categories of anesthesia machines exist: rebreathing systems and non-rebreathing systems. Rebreathing systems are so named because the gases exhaled by the patient are reintroduced into the breathing circuit. Non-rebreathing systems must be used on small patients, because the addition of one-way valves and carbon dioxide absorbers, required for a rebreathing circuit, introduce too high a resistance for the patients to overcome. In veterinary practice, non-rebreathing systems are used for cats and small dogs.

The most common non-rebreathing system, called a Bain Circuit, consists of a set of coaxial tubes, as seen in Figure 1. The inner tube, F, supplies the system with an oxygen-anesthesia gas mixture. The patient, P, inhales the fresh gas and then exhales into the reservoir tube, R. During exhalation, fresh gas is continuing to flow into the reservoir tube, pushing the expired gas out the end of the reservoir tube into the atmosphere or a scavenging system until the patient inhales again.

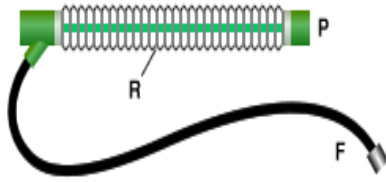


Figure 1. Bain Circuit [1]

Rebreathing systems allow some of the patient's expired gas to circulate back through the system, allowing less oxygen and anesthetic gases to be used. A schematic of a rebreathing circuit can be seen in Figure 2, and a photograph of a machine can be seen in Figure 3.

Rebreathing systems begin with oxygen supplied from the oxygen cylinder (1)<sup>1</sup> at a regulated pressure and flow rate into a precision vaporizer (2), which mixes the oxygen with the anesthetic gases at a concentration of 1.3% for isoflurane, a common anesthetic agent. This mixture then enters the circle system, the patient-end of the machine. Additionally, there is a vaporizer bypass, containing the oxygen flush valve (3), which is employed when it is necessary to quickly deliver oxygen to the patient without anesthesia. Once the anesthetic gas mixture, referred to as fresh gas flow, enters the circle system, it flows through a one-way valve (4) into the inspiratory breathing tube (5) before the Y-piece (6), which is connected to the patient (7). The gas mixture is inhaled by the patient, and then exhaled into the expiratory breathing tube (8). The gases then pass through another one-way valve (9) before returning to the circuit. These one-way valves ensure that the expired gas from the patient is treated before being inhaled again. After the expiratory one-way valve, the gases enter the adjustable pressure-limiting valve, known as the pop-off valve (10). The pop-off valve is adjusted to relieve excess gases to the scavenging system, which removes waste gas from the system without allowing any to enter the atmosphere, while keeping enough gas in the circuit to allow the reservoir bag (11) to partially inflate. Next, the expired gas enters a

---

<sup>1</sup> These numbers refer to the component labels in Figures 2 and 3

carbon dioxide absorbent canister (12) to remove carbon dioxide from the gas mixture. This treated expired gas then joins the fresh gas feed from the precision vaporizer and is again inhaled by the patient.

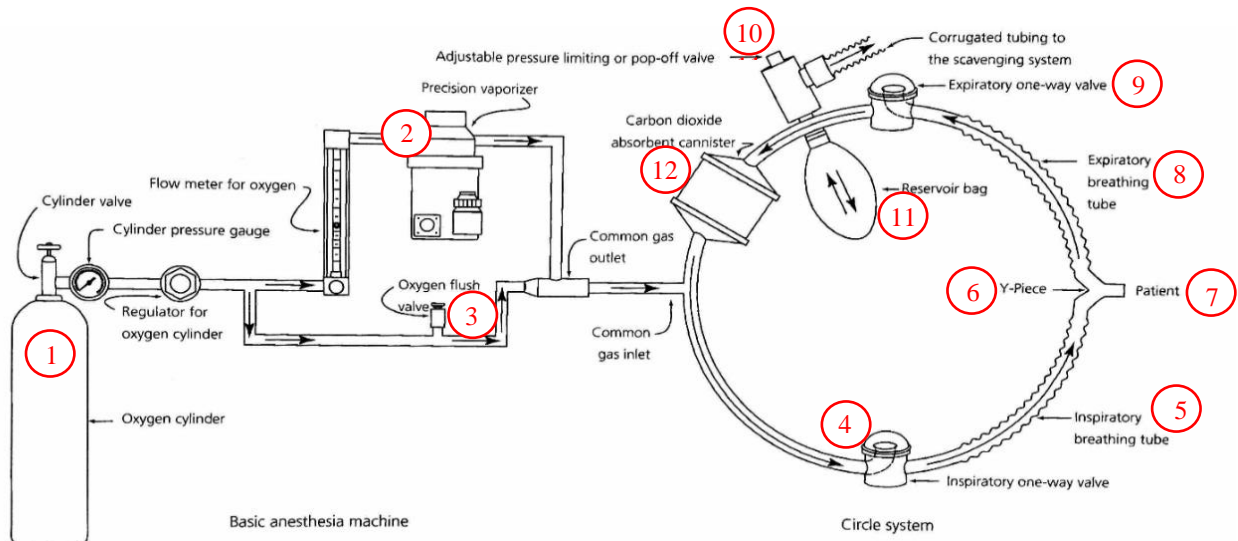


Figure 2. Basic Rebreathing Anesthesia Machine Schematic [1]

It is sometimes necessary to mechanically ventilate (i.e. manually breathe for) a patient under anesthesia. To do this, the pop-off valve must first be closed such that no gases leave the circuit, and then the reservoir bag is compressed, pushing the gas into the circle system and the patient's lungs. Because the pop-off valve is closed, there is no pressure regulation in the circuit during this process. Additionally, veterinarians sometimes fail to reopen the pop-off valve after mechanical ventilation, leading to over-pressurization of the breathing circuit and, without intervention, the patient's lungs. Lung injury due to elevated pressure is referred to as barotrauma. One common manifestation of barotrauma is pneumothorax, or a collapsed lung, which can be fatal. Peak airway pressures higher than 25 cm H<sub>2</sub>O should be avoided [2].

Cases of barotrauma occurring during anesthesia are widely documented, and some suggestions have been made to prevent future incidences. Dr. Bob Stein of Veterinary Anesthesia & Analgesia Support Group gives three reasons for the pop-off valve causing damage to a patient:

it was left closed after initially checking the system for leaks, it was left closed after mechanically ventilating a patient, or it was left partially closed to facilitate long term mechanical ventilation [3].

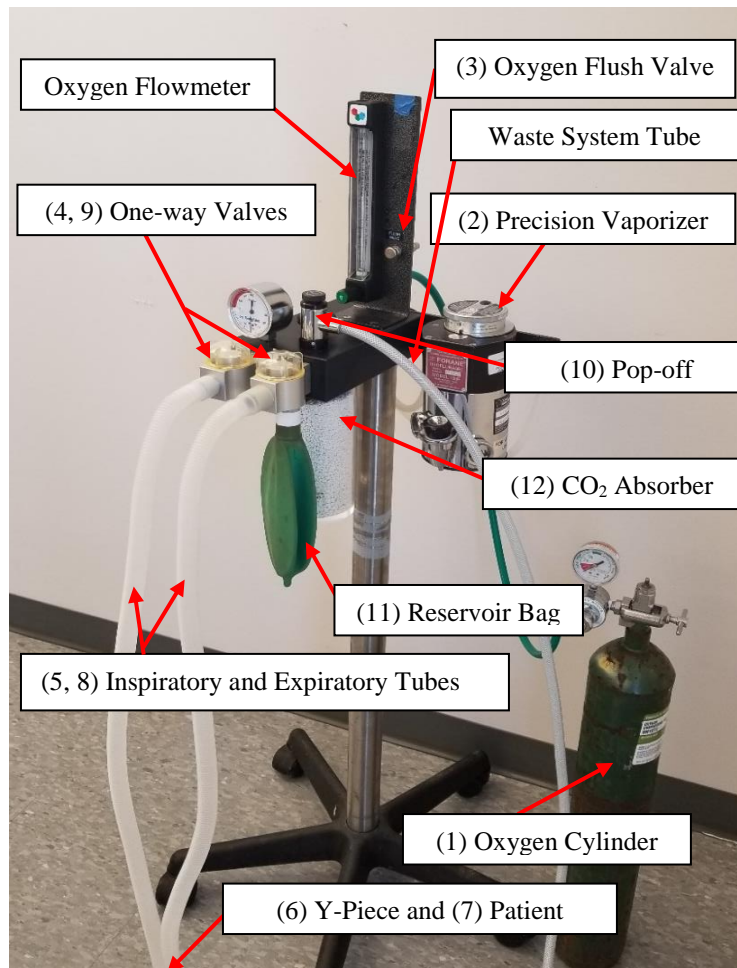


Figure 3. Rebreathing Anesthesia Machine Image

One documented case from the *Australian Veterinary Journal* describes the anesthetic death of a cat due to barotrauma. The pressure in the non-rebreathing circuit built up due to an accidental seal between the fresh gas line and the adapter to the patient, preventing the excess gas from leaving the circuit [4]. The *American College of Veterinary Surgeons* cite two additional cases, both involving cats under anesthesia. In one of these cases, a brass tube meant to discharge to the scavenging system was positioned in the tail of the reservoir bag, occluding the outflow of

excess gas. In the other case, the pop-off valve had been inadvertently left closed after mechanical ventilation. Because veterinary medicine does not require incidents to be recorded and published, it is likely there are many more similar occurrences that were unable to be found.

## 1.2 Safety Relief Valves

A safety relief valve (SRV) is a device designed to protect a component, system, or process by relieving pressure above a specified maximum allowable working pressure. SRVs fall into two categories: direct-spring operated (Figure 4) and pilot-operated. Additionally, instrumentation and controls can be added to direct-spring operated SRVs to regulate pressure in controlled safety pressure relief systems. Relief valves in veterinary anesthesia machines are direct-spring operated valves.

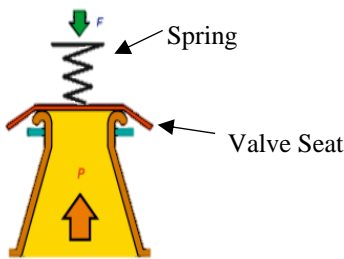


Figure 4. Simplified Diagram of Direct-Spring Operated SRVs [5]

As the name implies, opening and closing of direct-spring operated SRVs are regulated by a spring. The spring force, typically adjustable, and the area of the valve seat determine the pressure at which the valve will open. The force of the spring is given by

$$F_s = kx$$

where  $k$  is the spring constant and  $x$  is the displacement of the spring. The force of the pressure pushing up on the valve seat is given by

$$F_p = pA$$

where  $p$  is the pressure of the fluid in the valve and  $A$  is the area that the pressure acts on. When

$F_p = F_s$ , the valve opens, allowing the fluid to escape the circuit and the pressure to decrease. The spring force can be increased by applying a preset displacement, i.e. increasing  $x$ . This increases the force required to overcome the spring, and thus, the pressure required to overcome it. The pop-off valve in veterinary anesthesia machines is an adjustable direct-spring operated SRV. When the valve is adjusted to its closed position, the displacement,  $x$ , is at maximum. Adjusting the valve to a more open position decreases  $x$ , in turn decreasing the pressure required to open the valve.

### 1.3 Existing Solutions

Although often unimplemented, there are a few devices which can protect veterinary patients from barotrauma. Pop-off occlusion valves, seen in Figure 5a, are often recommended by veterinary anesthesiologists because they eliminate the need to close the pop-off valve [6], [3]. To mechanically ventilate a patient, the operator must depress a button on the occlusion valve, which restricts the exhaust side of the pop-off valve. Once the button is released, the valve is reopened, and the pop-off valve pressure does not need to be reset. If used properly, this prevents the pop-off valve from being left closed inadvertently. However, if the personnel are not properly trained and close the pop-off valve, the occlusion valve does not do anything to prevent rising pressure in the circuit. Since mechanical ventilation using a pop-off occlusion valve requires both hands (one to close the occlusion valve and one to squeeze the reservoir bag) and some patients need to be mechanically ventilated for extended periods of time, the veterinarian or veterinary technician may choose instead to close the pop-off valve to free one hand, endangering the patient. The cost of implementing one of these valves is about \$50.

Safety pop-off valves (Figure 5b) operate using the same principle as pop-off occlusion valves, but the “button,” or plunger in this case, is integral to the pop-off valve. This requires a full

replacement of the pop-off valve in the anesthesia system, and, like the occlusion valve, can be inconvenient for the anesthesia personnel.

The EMD safety valve (Figure 5c) can be placed either just after the inspiratory valve or just before the expiratory valve in the circle system and relieves excess gas at a set pressure. This valve was invented by a veterinarian and can be purchased online for \$175.

Another suggested modification of a non-rebreathing circuit introduces a positive end-expiratory pressure (PEEP) valve (Figure 5d). PEEP valves are designed to maintain a predetermined pressure level, but the reverse configuration of this valve relieves gas when the pressure in the circuit exceeds this value [7], [8]. The anesthetic circuit model is later used to compare the effectiveness and safety of the EMD valve and Reverse-PEEP valve.



Figure 5. Existing Solutions. a) Pop-Off Occlusion Valve [9]; b) Safety Pop-Off Valve [10]; c) EMD Safety Valve [11]; d) Reverse-PEEP Valve [8]



## 1.4 Relevant Patents

Several valves aiming to improve anesthesia systems for both humans and animals have been patented. One patent, the valve seen in Figure 6, improved upon the pop-off valves in 1971 by introducing the ability to discharge to a closed system. Previously, pop-off valves discharged to atmosphere, endangering the anesthesia personnel by exposing them to the anesthetic gases, affecting their motor function while performing surgery. This is a spring loaded valve which relieves gas either to a closed system or to the atmosphere when the pressure of the gas over the valve seat reaches the spring set force, which is adjustable [12]. This valve appears to be what is considered a standard pop-off valve.

The patented Dual Valve [13], seen in Figure 7, addresses the complications of leaving a pop-off valve closed. This spring-loaded valve contains a plunger that, when depressed, pushes against the valve seat. This causes the valve to remain closed, and mechanical ventilation to be performed. Upon release, an additional spring resets the plunger back to its original position, and the pop-off valve can operate as before [13].

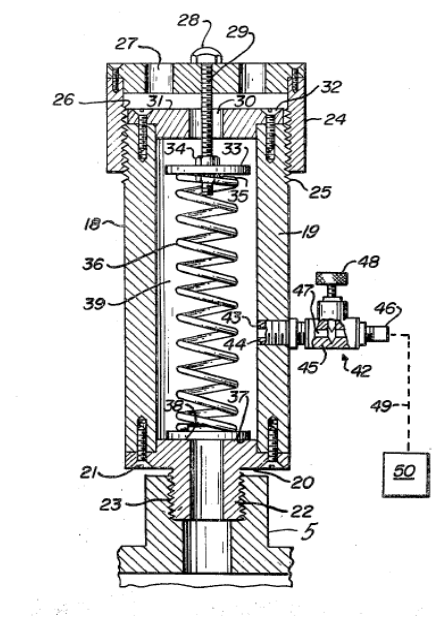


Figure 6. Closed Exhaust Discharge System [12]

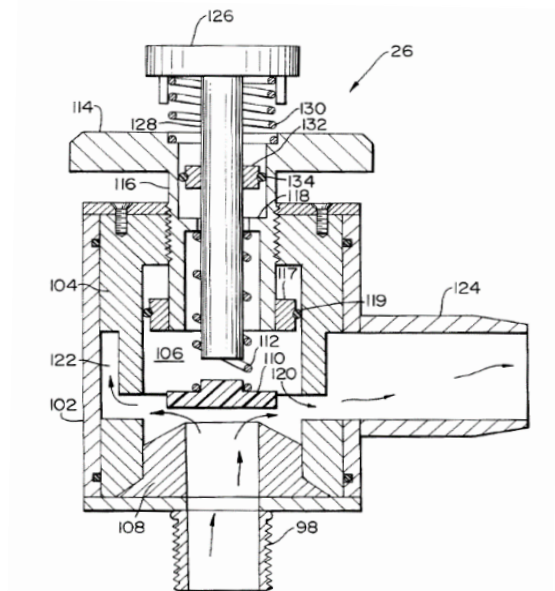


Figure 7. Dual Valve [13]

A veterinary-specific valve patent (Figure 8) is designed to connect to a non-rebreathing system and contains a spring-loaded valve with three ports. One port of the valve is connected to the expiratory tube of the patient, another to the reservoir bag, and the third to atmosphere or a scavenging system. This valve acts similarly to the aforementioned valve with the plunger when manually ventilating a patient. Mechanical ventilation is permitted as long as the button on the top of the valve is depressed [14]. The functionality of the latter two patents is realized in the Supera Safety Pop-off Valve pictured in Figure 4b.

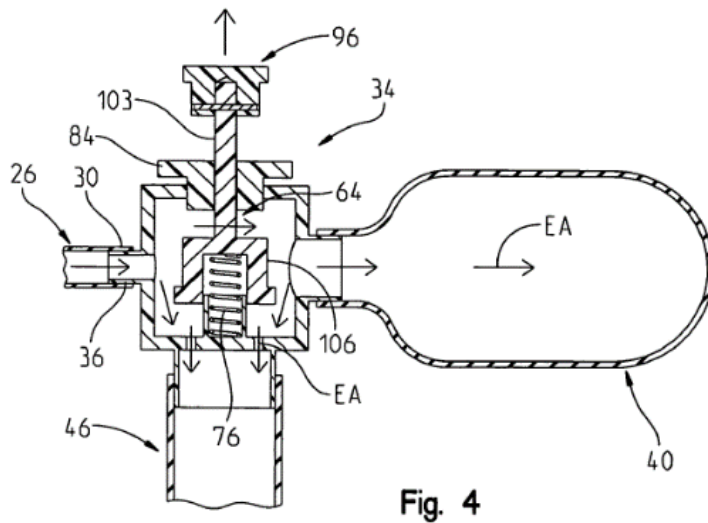


Figure 8. Ventilation Valve [14]

### 1.5 Modeling of Anesthetic Circuits

J. G. C. Lerou and L. H. D. J. Booij [15] developed a model for the administration of inhalation anesthesia. In this model, ventilation is treated as continuous, not cyclical, and the partial pressures of gases at various stages in the cycle are used to determine total pressure, flows, and gas exchange rates. The anesthetic circuit used in this model is a rebreathing circuit with a standing bellows in place of the pop-off valve typically found in veterinary circuits. The block diagram in Figure 9 for this model splits the anesthetic circuit into an inspiratory subsystem, two expiratory subsystems, the patient's alveolar space, and dead space. The direction of flow,  $\dot{V}$ , is

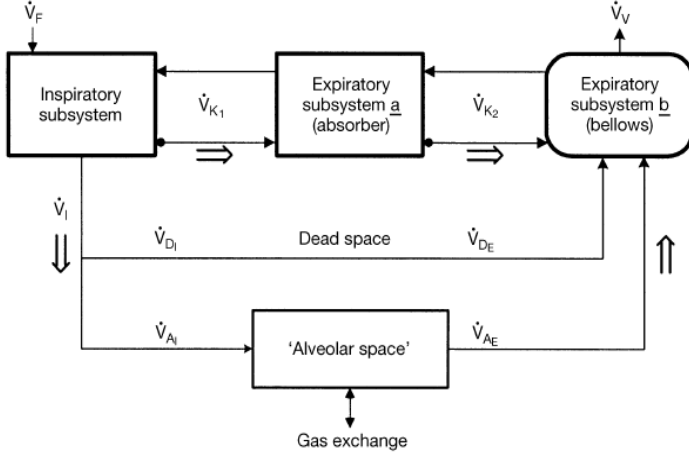


Figure 9. Anesthetic Circuit System Model [15]

depicted both in the direction of rebreathing and in the opposite direction, in the case of a non-rebreathing conditions.

Assuming ideal gas behavior in the circuit, partial pressure of a gas is given by

$$P_{S_i} = RT_S \frac{n_{S_i}}{V_S}$$

where  $P_{S_i}$  is the partial pressure of the  $i^{th}$  gaseous species of a subsystem,  $S$ ,  $R$  is the ideal gas constant,  $T_S$  is the temperature of the subsystem, and  $n_{S_i}$  is the amount of the substance in moles.

Summing the partial pressures of all components gives the total pressure of the subsystem,

$$P_S = \sum_{i=1}^N P_{S_i}$$

where  $N$  is the number of gaseous species in a subsystem.

The partial pressures in the lung are related by the following relation [15]:

$$P_{A_{O_2}} = 0.209 \left( P_B - P_{A_{H_2O}} \right) - \frac{P_{A_{CO_2}}}{R_n} + \frac{P_{I_{O_2}}}{P_B} \left( \frac{P_{A_{CO_2}}}{R_n} - P_{A_{CO_2}} \right)$$

where A, B, and I refer to the alveolar subsystem, the initial condition of dry room air, and the inspiratory subsystem, respectively.

Flow is related to subsystem pressure by

$$\dot{V}_{S_1 \rightarrow S_2} = \frac{P_{S_1} - P_{S_2}}{\left( \frac{P_{S_1} \Delta t}{1.25 V_{S_2}} \right)}$$

where  $\Delta t$  is the time step used for integration. This model was found to agree with the dynamics of an anesthetic circuit [15].

A model of the isolated respiratory system comes from Mešić et al [16], who simulated the artificially ventilated lung in humans. A second order linear model is used to represent the dynamic compliance of the respiratory system, and a nonlinear flow and volume dependent resistance model is used, shown in the block diagram in Figure 10. The variables in the block diagram are listed in Table 1.

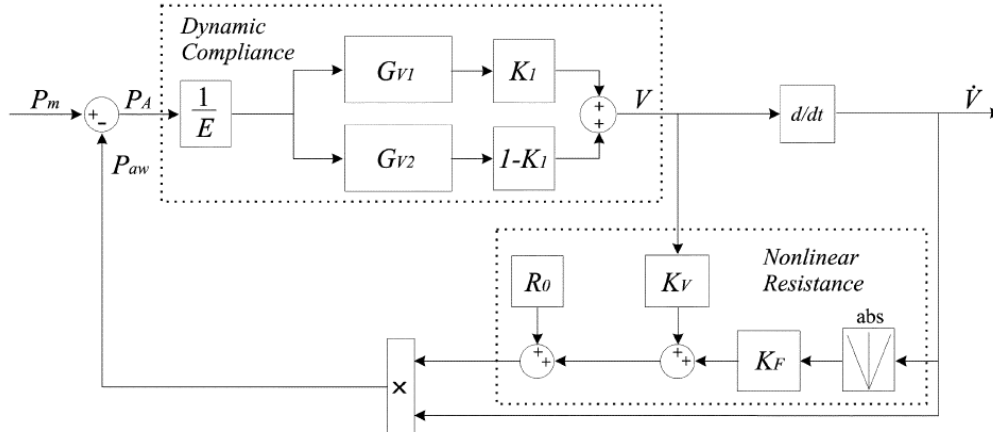


Figure 10. Mešić et al Complete Model of Respiratory System [16]

To validate the model, values for  $K_1$  and  $\tau_2$  were taken from the literature and  $\tau_1$  was taken to be sufficiently small [16]. Values for  $R_0$ ,  $K_V$ , and  $K_F$  were found from data taken from artificially ventilated patients [16], and initial values were found using the following simplified equation:

$$P_m = EV + (R_0 + K_V V + K_F |\dot{V}|) \dot{V} \quad [16]$$

The measured and simulated flows for this model from Mešić et al were found to be consistent [16].

Table 1. Variables from Mešić et al Model [16]

Variable	Description
$P_m$	Mouth pressure [kPa]
$P_A$	Alveolar pressure [kPa]
$P_{aw}$	Pressure exerted in the airways [kPa]
$E$	Lumped elasticity of the lung and thorax [ $l^{-1}kPa$ ]
$\tau_1$	Time constant due to quick changes in lung volume [s]
$G_{V1}$	Transfer function dependent on $\tau_1$ [-]
$\tau_2$	Time constant due to viscosity [s]
$G_{V2}$	Transfer function dependent on $\tau_2$ [-]
$K_1$	Viscosity ratio coefficient [-]
$R_0$	Laminar flow resistance [ $kPa s l^{-1}$ ]
$K_V$	Volume resistance coefficient [ $kPa s l^{-2}$ ]
$K_F$	Flow resistance coefficient [ $kPa s^2 l^{-2}$ ]
$V$	Lung volume increment above functional residual capacity [l]
$\dot{V}$	Airflow as the derivative of lung volume with respect to time [ $l s^{-1}$ ]

A block diagram of the anesthetic circuit is seen in Figure 11. The gas composition is not taken into consideration. Input flow,  $\dot{V}_1$ , after being added to the flow remaining in the circuit, passes through the inspiratory one-way valve,  $R_{CV}$ , and the inspiratory corrugated tube,  $R_T$ . The flow then enters the patient,  $G_P$ . The gases expired by the patient pass again through a corrugated tube and the expiratory one-way valve. The gas flows past the reservoir bag,  $C_{Res}$ , and then the pop-off valve,  $R_{PO}$ . The pop-off valve removes some of the gases from the circuit. The remaining

flow enters the carbon dioxide absorber before returning to the circuit with the fresh gas flow.

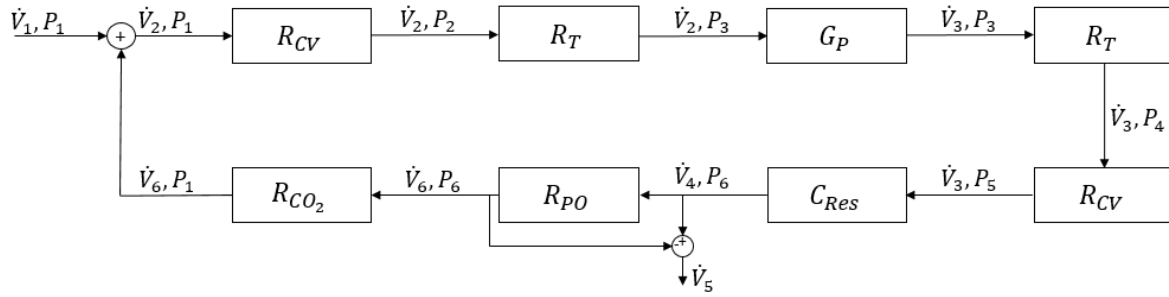


Figure 11. Block Diagram of Rebreathing Anesthesia Machine

## 1.6 Simscape

Simscape, within the Simulink software, is used to model physical systems. Companies such as Airbus, Volvo, and Sandia National Laboratories have used Simscape to model their physical systems to make design and control decisions [17]. Unlike Simulink models, where a system diagram represents a set of mathematical equations, Simscape models are comprised of physical component blocks. This allows for system modeling without state equation derivation. Physical component models are connected at their ports by physical signal lines. A component block has as many ports as it has energy exchanges with the system. Each port specifies two variables: a *Through* variable and an *Across* variable. A *Through* variable is one that is measured in series to the element, i.e. flow rate, and an *Across* variable is one that is measured in parallel to the element with a reference, i.e. pressure. These two variables define the energy flow for a port.

Consider the behavior of the hydraulic cylinder in Figure 12. Ports A and B have *Through* variables  $q_1$  and  $q_2$  for flow rate into or out of the chambers and *Across* variables  $p_1$  and  $p_2$  for the pressure at the port. Port R, in the mechanical translation domain, has *Through* variable  $v_3$  for rod velocity and *Across* variable  $F_3$  for rod force. This component can be defined by its characteristic equations, relating the *Through* and *Across* variables through the piston area. Simscape has been used for a variety of engineering solutions.

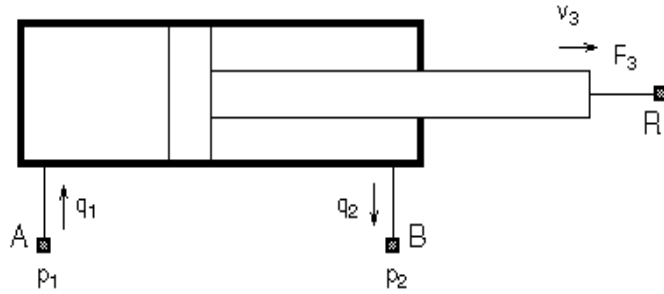


Figure 12. Hydraulic Cylinder [18]

## 1.7 Motivation

Dr. Anderson da Cunha of the LSU School of Veterinary Medicine contacted the College of Engineering to address the risk of barotrauma during inhalation anesthesia. Because the Veterinary School trains inexperienced students to operate these machines, it is important that precautions be taken to prevent injury. Since the time of original inquiry, the Veterinary School has begun to use the EMD Valve for this purpose. A Simscape Fluids model was developed to simulate the veterinary anesthetic system to compare the performance of two pressure regulation solutions: the EMD valve and the PEEP valve in reverse orientation. Based on the results for the model, one of the two solutions is recommended.

## Chapter 2. Methodology

This chapter outlines the experimental configurations used to collect data for the model as well as methods used to analyze and report the data. A case is made for using the built-in Simscape Fluids library for this gas system, and the full Simscape model is explained.

### 2.1 Experimental Methods

To model the system, pressure and flow data were taken for each component to serve as a reference when setting parameters for the Simscape component blocks for these components. Pressure values for were found using Setra 264 pressure transducers, which were powered by an HP E3630A DC Power Supply unit. The data were recorded using an NI USB-6210 DAQ device and LabVIEW. For each reading, input oxygen flow rate was kept constant using a Porter Instruments GL-616 oxygen flowmeter. Six (6) test flow rates were used in the characterization of each component: 0.2, 0.6, 1, 2, 3, and 4 liters per minute (LPM). Table 2 shows the configuration parameters for the three following measurement configurations.

The pressure drop was measured across circuit components that act as fluid resistances, such as the one-way valves, the corrugated tubes, and the carbon dioxide absorber for each flow rate. The experimental setup can be seen in Figure 13. As described later, this data was used to develop characteristic relations for the model blocks.

Table 2. Summary of Experimental Measurement Parameters

	Transducer(s)	Accuracy	Sample Rate	Measurements
Configuration 1	0.1-inH <sub>2</sub> O	±1.0%	100 Hz	10
Configuration 2	25-inH <sub>2</sub> O	±0.25%	100 Hz	5
Configuration 3	25-inH <sub>2</sub> O	±0.25%	100 Hz	10
	5-inH <sub>2</sub> O	±0.25%	100 Hz	10



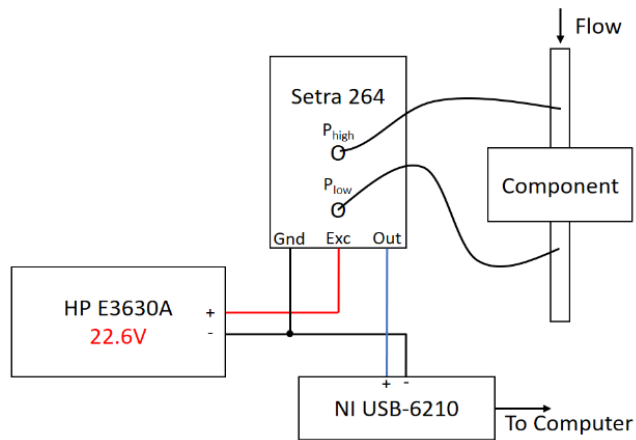


Figure 13. Experimental Setup Schematic 1

To characterize the behavior of the reservoir bag, the pressure response over time for each test flow rate was found. As shown in Figure 14, the response to a constant flow input was measured. As seen in the figure, a  $244\ \Omega$  resistor was used to convert the current output to a voltage, able to be read by the DAQ unit. These curves are later compared to the pressure response of the built-in gas-charged accumulator block used to represent the reservoir bag in the model.

Relief valves such as the pop-off valve, the reverse-PEEP valve, and the EMD valve do not only act as a fluid resistance, but also relieve pressure. For this reason, these components were attached to the reservoir bag to find the pressure response over time as well as the drop in pressure across the component at various pressure values. The configuration for these measurements is seen in Figure 15. For the pop-off valve, a third variable, openness, is introduced; the response was taken for five (5) degrees of openness of the valve. An image of the test configuration for the pop-off Valve is seen in Figure 16. The one-way valve was incorporated for the pressure response tests of the relief valves to ensure that the flow entering the test valve came only from the anesthesia machine at the regulated flow rate. As is seen later, these measured pressure responses are used to define the parameters for the build-in relief valve blocks in Simscape.

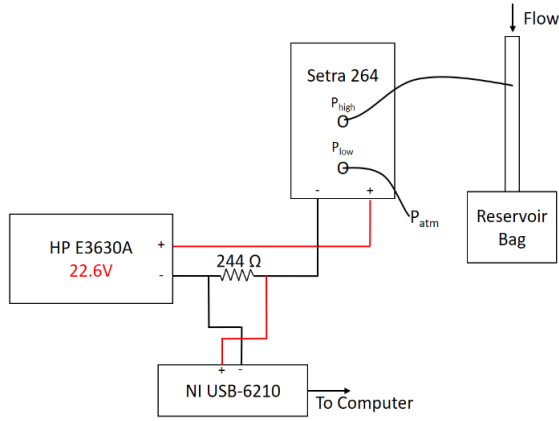


Figure 14. Experimental Setup Schematic 2

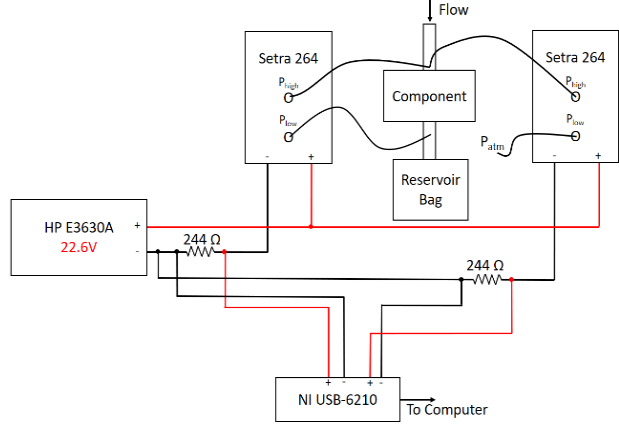


Figure 15. Experimental Setup Schematic 3

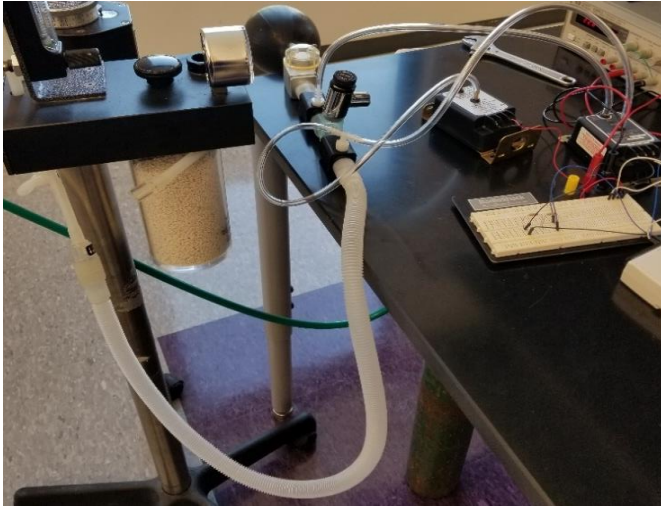


Figure 16. Experimental Setup for Pop-off Valve

For both the reservoir bag pressure response and the relief valve pressure responses, the pressure at each time, normalized to the same pressure at a given point, were averaged and later used as a reference for the behavior of the model components. In reported values and figures of the measured values, a confidence interval of 95% based on the Student's *t* distribution method, developed by William Gosset, is included [19]. Additionally, R-square values are reported with curve-fits to measured data, calculated by the following equation:

$$R\text{-square} = 1 - \frac{SSE}{SST} \quad [20]$$

where SSE is the sum of the squares of the errors between the data and the regression, and SST is the sum of the squares about the mean of the data set. Therefore, R-square values range from 0 to 1, with those close to 1 representing that the regression adequately accounts for the variation of the dependent variable with respect to the independent variable. However, in the case of regressions with multiple independent variables, such as the pressure drop of the relief valves, the degrees of freedom adjusted R-square statistic should be used. The adjusted R-square value is defined as

$$\text{adjusted } R\text{-square} = 1 - \frac{SSE(n-1)}{SST(v)} [20]$$

where  $n$  is the number of response values and  $v$  is the difference between  $n$  and the number of coefficients in the regression expression [20]. Adjusted R-square values also range from 0 to 1, with values close to 1 representing a better fit.

## 2.2 Simscape Fluids

Simscape includes a Gas Foundation library, but the components are rudimentary, including resistances and sources, but not developed components such as valves. There is also a Simscape Fluids library, which employs a set of more complex components, such as pumps, valves, and accumulators. It is therefore desired to use the Simscape Fluids built-in library so as to begin with higher level modeling. To use the Simscape Fluids library for a gas system, the gas flow being studied must be reasonably approximated as having incompressible flow. To determine this, the Mach number,  $M$ , of the gas flow must be calculated, [21]

$$M = \frac{v}{a}$$

where  $v$  is the velocity of the flow, and  $a$  is the speed of sound for that fluid flow. The flow velocity is determined by dividing the flow rate by the cross-sectional area through which it flows. For a

maximum 4 LPM flow rate and a 15 mm diameter tube characteristic of anesthesia systems, this gives a flow velocity of 0.38 m/s. The speed of sound,  $a$ , is determined by the equation [21]

$$a = \sqrt{\gamma RT}$$

where  $\gamma$ , specific heat ratio and  $R$ , the gas constant are assumed to be those for oxygen, i.e. 1.4 and 0.2598 kJ/kgK, respectively, and  $T$  is the body temperature of a dog in Kelvin, 311 K [22]. This results in a speed of sound of 340 m/s, giving a Mach number of 0.0011. Because this value is much smaller than 0.3, the flow can be approximated as incompressible, and, thus, modeled using Simscape Fluids.

### 2.3 Model Description

The Simscape Fluids model of the anesthesia system can be seen in Figure 17. The oxygen tank, flow regulator, and precision vaporizer are treated as a flow source. The oxygen flush valve is omitted because it is only used in cases of emergency, and never when a patient is attached to the machine [23]. The flow enters the inspiratory one-way valve and then reaches the patient. The expired gas from the patient then flows through the expiratory one-way valve before flowing past the reservoir bag, modeled as a gas-charged accumulator. The gas then flows through the pop-off valve, modeled as a pressure relief valve and a fluid resistance, and then through the carbon dioxide absorber. This flow joins with that of the flow source and returns to the breathing circuit. When the model is run with the EMD and Reverse-PEEP valves, a fluid resistance and a pressure relief valve are added between the patient and one-way valve, as seen in Figure 18.

The Solver Configuration block, seen in Figure 19, defines parameters for the solver. For the anesthesia model, all default parameters were used. Figure 20 shows the Custom Hydraulic Fluid block, which is used to specify the fluid characteristics. The Clock block, shown in Figure 21, is used to record the time steps of the simulation, and is connected to a To-Workspace block

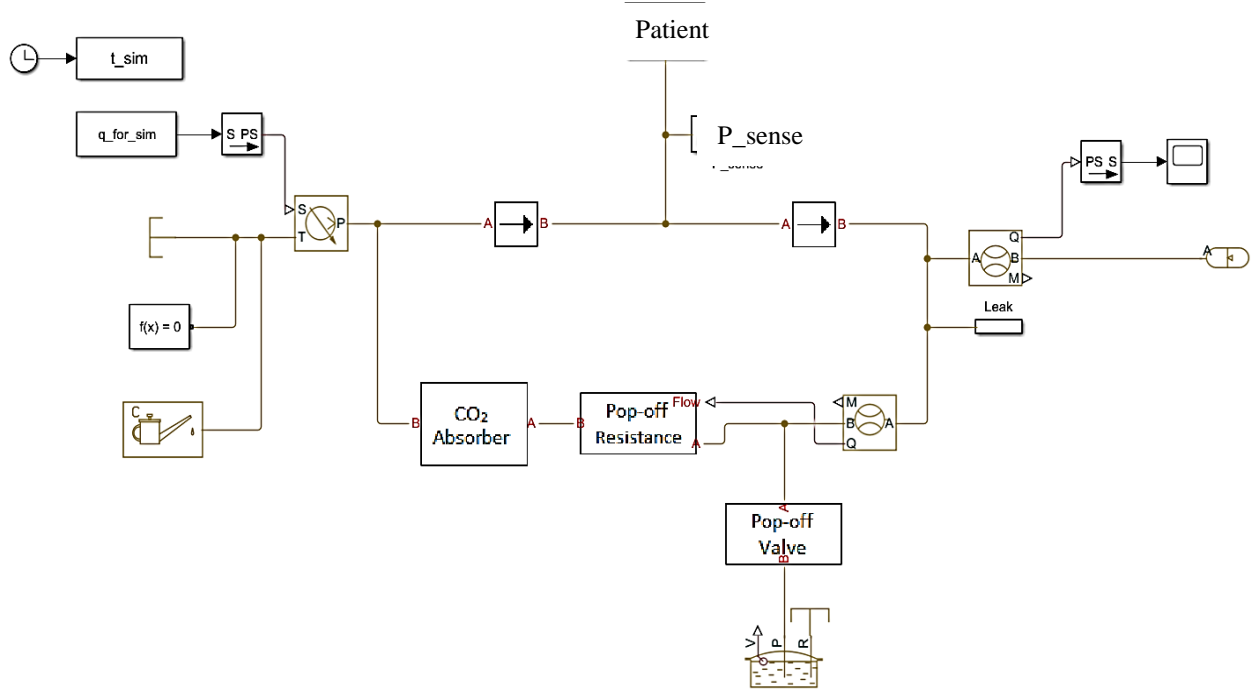


Figure 17. Simscape Model of Veterinary Anesthesia System

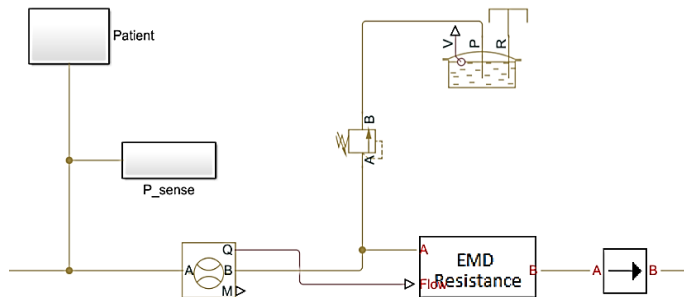


Figure 18. EMD Valve Addition

so it can be used for analysis. The oxygen flow source connection is seen in Figure 22. The Hydraulic Flow Source block is connected to a Simulink to Physical Signal block so it can interpret the flow setting from the Constant block. The Constant block allows a variable value from the MATLAB workspace to be input to the Hydraulic Flow Source block. The Gas-Charged Accumulator block used to model the reservoir bag is shown in Figure 23. This block does not consider fluid compressibility, hydraulic resistance at inlet, inertia, or damping. The behavior of the gas is considered to be a polytropic process.

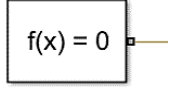


Figure 19. Solver Configuration Block



Figure 20. Custom Hydraulic Fluid Block

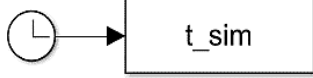


Figure 21. Clock Block

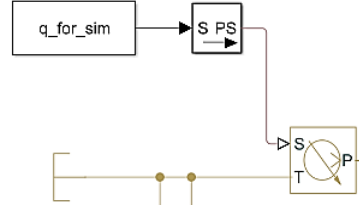


Figure 22. Oxygen Flow Source Connection

Figure 24 shows the Pressure Relief Valve block, which is used for the pop-off, EMD, and Reverse-PEEP valves. The flow rate in  $\text{m}^3/\text{s}$  through the valve is determined by the equation

$$q = C_D A \sqrt{\frac{2}{\rho} \frac{p}{(p^2 + p_{cr}^2)^2}}$$

where  $C_D$  is the flow discharge coefficient,  $A$  is the valve opening area in  $\text{m}^2$ , which is a function of pressure,  $\rho$  ( $\text{kg}/\text{m}^3$ ) is the fluid density,  $p$  is the pressure in the circuit in Pa, and  $p_{cr}$  is the minimum pressure for turbulent flow in Pa, based on the set pressure, regulation pressure, and pressure ratio at transition between laminar and turbulent flow. The set pressure of the valve, also known as the cracking pressure, is the pressure at which it first begins to open. The valve opening area at pressures lower than the set pressure is  $A_{leak}$ , or the closed valve leakage area. After the valve reaches the set pressure, the valve opening area increases linearly with pressure until it reaches  $A_{max}$  at  $p_{max}$ , or the sum of the set pressure and the regulation pressure. For the EMD valve and the pop-off valve at settings of 360, 540, and 720 degrees, valve opening dynamics are included in the block. In this case, the opening area of the valve is determined by the equation

$$\frac{dA_{inst}}{dt} = \frac{A(p) - A_{inst}}{\tau}$$



Figure 23. Gas-Charged Accumulator Block



Figure 24. Pressure Relief Valve Block

where  $A(p)$  is the calculated area as a function of pressure,  $A_{inst}$  is the instantaneous area, and  $\tau$  is the valve opening time constant.

Figure 25 shows the connection of the pop-off valve to the system. The Hydraulic Flow Sensor block is used to sense the total flow before gases are relieved to determine the pressure drop across the valve in the pop-off Resistance block. The pop-off valve block uses the same equations as the built-in Pressure Relief Valve block, but allows the parameters for different settings of the physical pop-off valve to be contained within one block. The block does not, however, incorporate the valve opening characteristics needed for pop-off valve settings of 360 degrees and above, so the built-in block is used under those conditions.

As seen in Figure 17, some of the component blocks are subsystems. Figure 26 shows the Patient subsystem. The patient is modeled simply as a sinusoidal flow source with an amplitude of 1 LPM and a 10 second period. Although this does not accurately represent the flow characteristic of respiration, it does introduce a periodic flow with accurate amplitude and frequency or respiration rate. The Simulink sinusoidal signal source is connected to a Simulink to Physical Signal block to allow the signal to be read by the Simscape Hydraulic Flow Source block. The Hydraulic Flow Source block is connected to the hydraulic reference block and then to the anesthetic circuit at port 1 of the subsystem. The Pressure Sensor Subsystem, seen in Figure 27, connects the point in the anesthesia system at subsystem port 1 to the Hydraulic Pressure Sensor block. The Hydraulic Pressure Sensor Block is then connected to hydraulic reference, or atmospheric pressure to calculate the gauge pressure in the system. The output passes through a

Physical Signal to Simulink block to be output in a To-Workspace block for analysis, as well as a Scope block to view the pressure behavior within Simscape.

Lastly, the leak subsystem (Figure 28) is comprised of two pressure-relief valves in parallel, venting to a reservoir at atmospheric pressure. This was added when comparing the

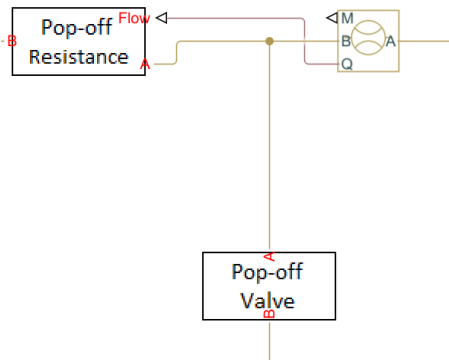


Figure 25. Pop-off Valve Connection

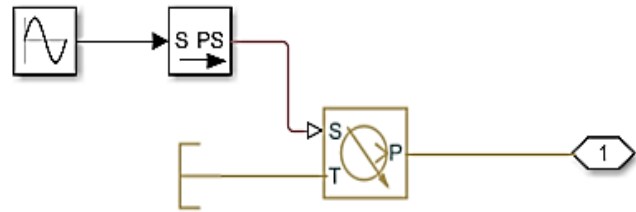


Figure 26. Patient Subsystem

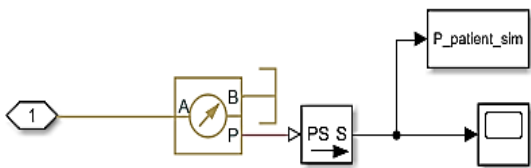


Figure 27. Pressure Sensor Subsystem

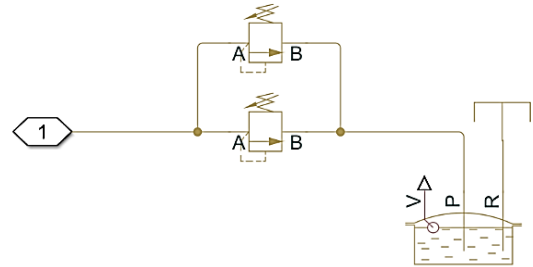


Figure 28. Leak Subsystem

behavior of flow entering the Gas-Charger Accumulator block in Simscape to the analogous data collected of flow entering the reservoir bag, because the real system did not keep pressure as the model did. The resulting behavior can be seen in the next section.

The model was run using a variable time step and Simscape's automatic solver selection of ode123t, which is used for moderately stiff differential-algebraic systems of equations using the trapezoidal rule of integration.



### Chapter 3. Results and Discussion

The pressure drop for each of the six (6) test flow rates for the one-way valve, carbon dioxide absorber, and corrugated tube are seen in Table 3. Because the pressure values for the corrugated tube are minimal, most of them too small to be read by the transducer, the tubes are excluded from the model. The dependency of this data was reversed to find a relation for one-way valve flow rate as a function of differential pressure. Because there is no negative direction flow in the one-way valve, an exponential fit was chosen, keeping flow values close to 0 for low and negative pressure values. The curve fit and data can be seen in Figure 29. Figure 30 shows the measured data and curve fit of the differential pressure across the carbon dioxide absorbent canister as a function of flow rate. Because the pressure drop simply changes direction when flow is reversed, the data points were reflected across  $y = -x$  to find the relation. The R-square values for the one-way valve and carbon dioxide absorber are 0.8993 and 0.9996, respectively.

Table 3. Pressure Drop Across Circuit Components for Various Flow Rates

Flow Rate (LPM)	One-way valve Pressure Drop (Pa)		CO <sub>2</sub> Absorber Pressure Drop (Pa)		Corrugated Tube Pressure Drop (Pa)	
	Measured	Model	Measured	Model	Measured	Model
0.2	$17.3 \pm 0.3$	13.70	$1.2 \pm 0.3$	1.18	$0.00 \pm 0.05$	-
0.6	$18.4 \pm 0.3$	18.09	$3.5 \pm 0.3$	3.53	$0.00 \pm 0.05$	-
1	$19.3 \pm 0.3$	20.14	$5.5 \pm 0.3$	5.89	$0.00 \pm 0.05$	-
2	$21.9 \pm 0.3$	22.92	$11.4 \pm 0.3$	11.78	$0.00 \pm 0.05$	-
3	$23.6 \pm 0.3$	24.54	$17.6 \pm 0.4$	17.67	$0.00 \pm 0.05$	-
4	$26.1 \pm 0.3$	25.70	$23.9 \pm 0.3$	23.55	$5.0 \pm 0.3$	-

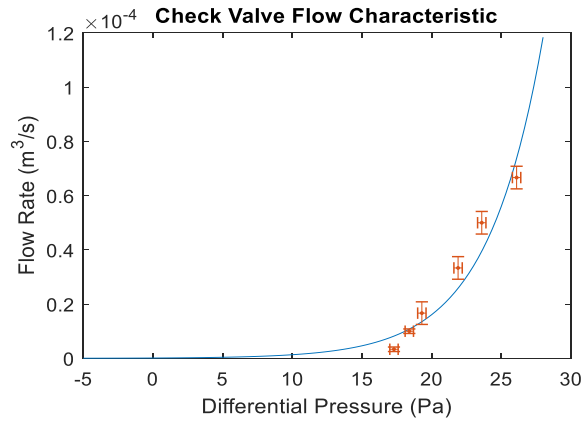


Figure 29. One-way Valve Flow Characteristic

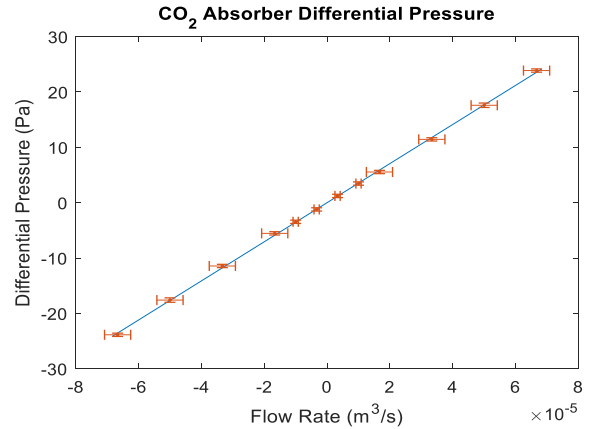


Figure 30. CO<sub>2</sub> Absorber Pressure Drop

Because the fluid resistance is a function of both flow rate and circuit pressure for the Pop-off Valve, EMD Valve, and Reverse-PEEP Valve, the measured pressure drop across the valves was passed through a low-pass filter and plotted against the flow rate and the circuit pressure. A polynomial relation of degrees 1 in pressure and 3 in flow rate was found after removing outlier values using MATLAB's curve fitting toolbox for each valve and each pop-off valve position. The plot for the pop-off valve at 0 degrees is seen in Figure 31, and the plots for the other positions of the pop-off valve as well as the PEEP and EMD Valves can be seen in Figures 32-37 on the following page. The outlier values excluded from the curve fit in Figure 31 are marked in red. These points were excluded because they are from only one of the five data recordings for this flow rate which reached a higher pressure than the rest, and, thus, are not averaged values.

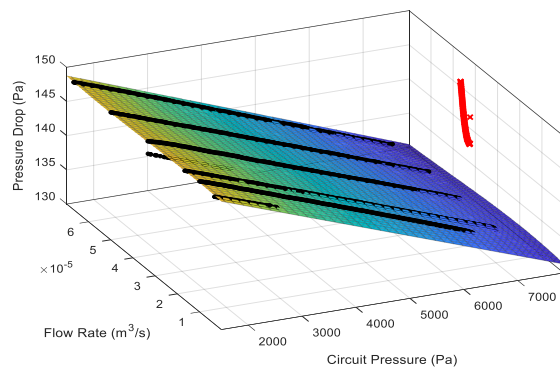


Figure 31. Pressure Drop Across Pop-off Valve set to 0 degrees

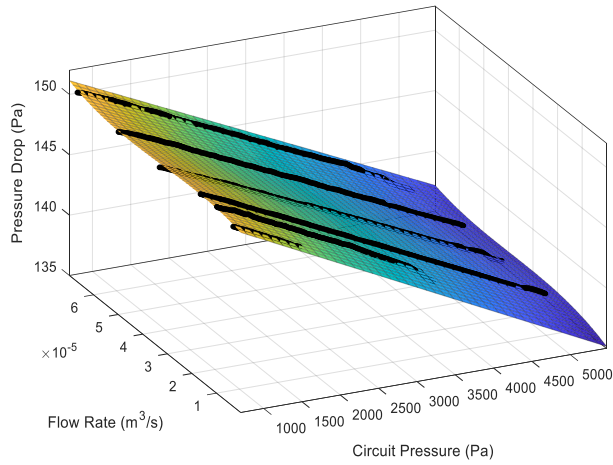


Figure 32. Pressure Drop Across Pop-off Valve set to 180 degrees

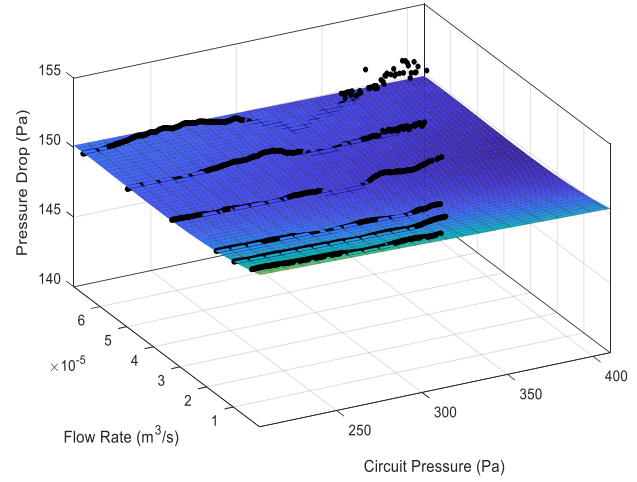


Figure 33. Pressure Drop Across Pop-off Valve set to 360 degrees

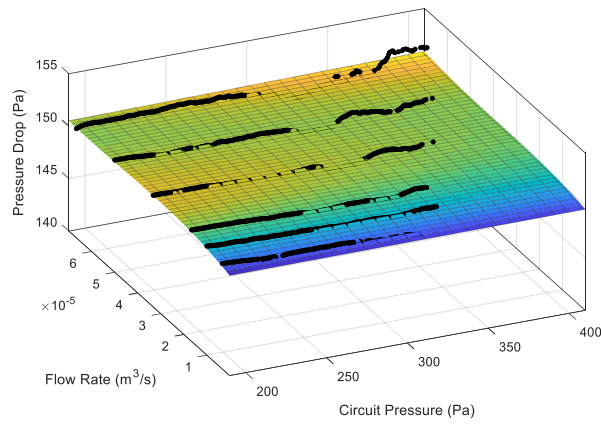


Figure 34. Pressure Drop Across Pop-off Valve set to 540 degrees

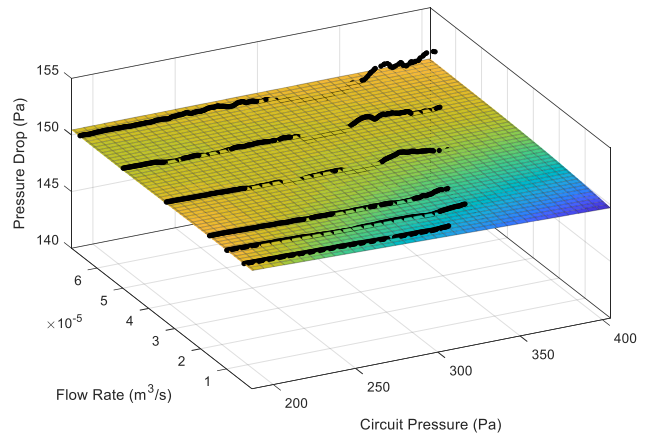


Figure 35. Pressure Drop Across Pop-off Valve set to 720 degrees

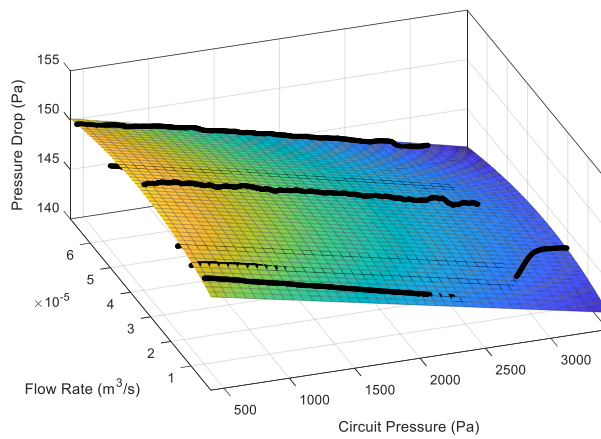


Figure 36. Pressure Drop Across EMD Valve

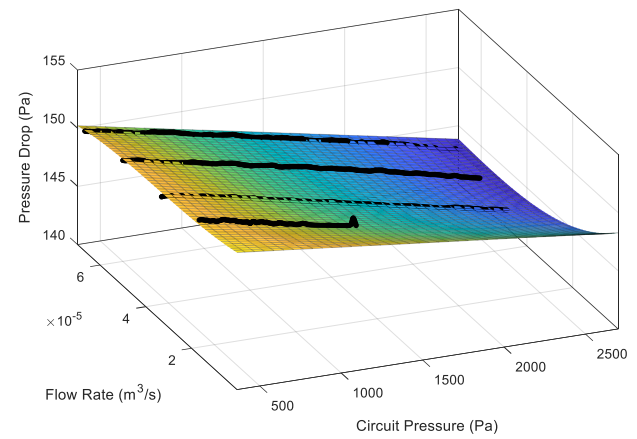


Figure 37. Pressure Drop Across Reverse-PEEP Valve

Table 4 shows the Adjusted R-square values of the resulting curve fits. The low Adjusted R-square values for the pop-off valve at positions 360, 540, and 720 degrees is explained by the fact that the valve chatters at opening pressure for these degrees of openness. This means that the opening area of the valve is fluctuating, causing the resistance of the fluid passing through the valve to fluctuate. As is seen later, these three degrees of openness behave almost identically, and the position with the most acceptable fit is used to represent all three positions.

Table 4. Adjusted R-square Values for Valve Pressure Drop Regressions

Valve	Adjusted R-square
Pop-off Valve 0°	0.9972
Pop-off Valve 180°	0.9986
Pop-off Valve 360°	0.6311
Pop-off Valve 540°	0.5399
Pop-off Valve 720°	0.1067
EMD Valve	0.8666
PEEP Valve	0.9884

The reservoir bag was modeled using the built-in gas-charged accumulator block. The parameters of the accumulator block were varied, and the response to a constant flow input for each test flow rate was plotted against the pressure response found experimentally. The model used to find the values is seen in Figure 38. A small leak, modeled as two pressure-relief valves in parallel was added to the circuit to fit more closely to the actual system. The pressure response of the reservoir bag and leak for the six (6) test flow rates can be seen in Figure 39. The calculated uncertainty of the average pressure response is indicated by yellow error bars.

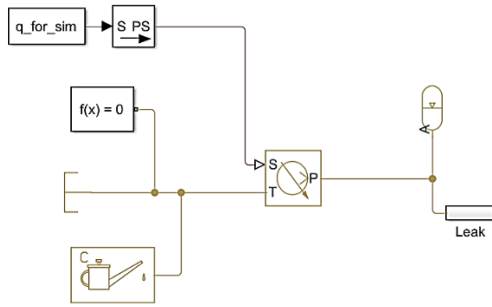


Figure 38. Reservoir Bag Test Model

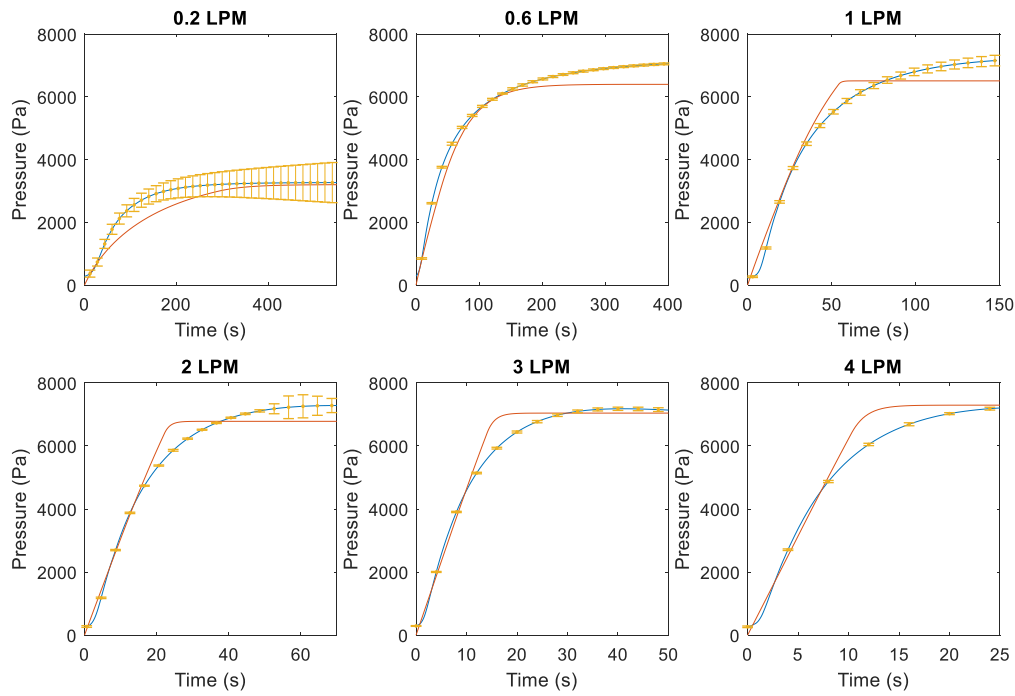


Figure 39. Experimental and Simulated Pressure Response of Reservoir Bag at Various Flow Rates

For the pop-off valve, EMD Valve, and Reverse-PEEP Valve blocks, a pressure relief valve was attached to the circuit containing the previously attained reservoir bag. Additionally, the one-way valve block and fluid resistance block corresponding to the valve were added to the circuit to fully capture the experimental conditions. Figure 40 shows the Simscape model that was used, and the results for each valve and each pop-off valve position are seen in Figures 41-47. The horizontal purple line indicated the maximum allowable pressure in the circuit, 25 cmH<sub>2</sub>O or 2450 Pa.

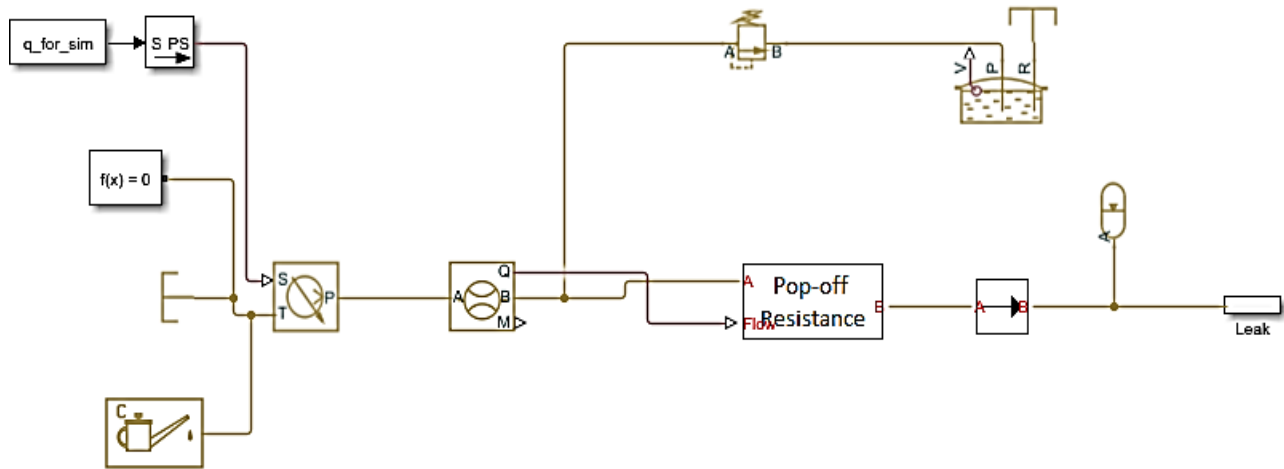


Figure 40. Relief Valve Test Model

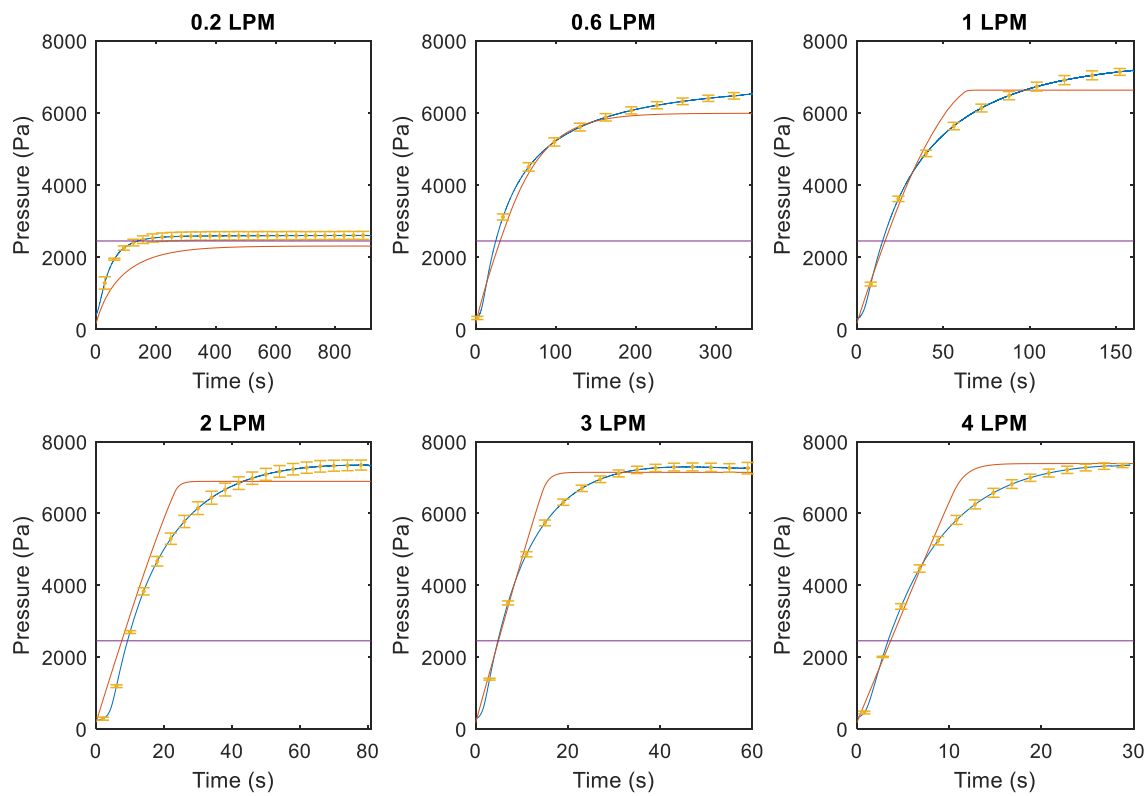


Figure 41. Experimental and Simulated Pressure Response of Pop-off Valve at 0 degrees at Various Flow Rates

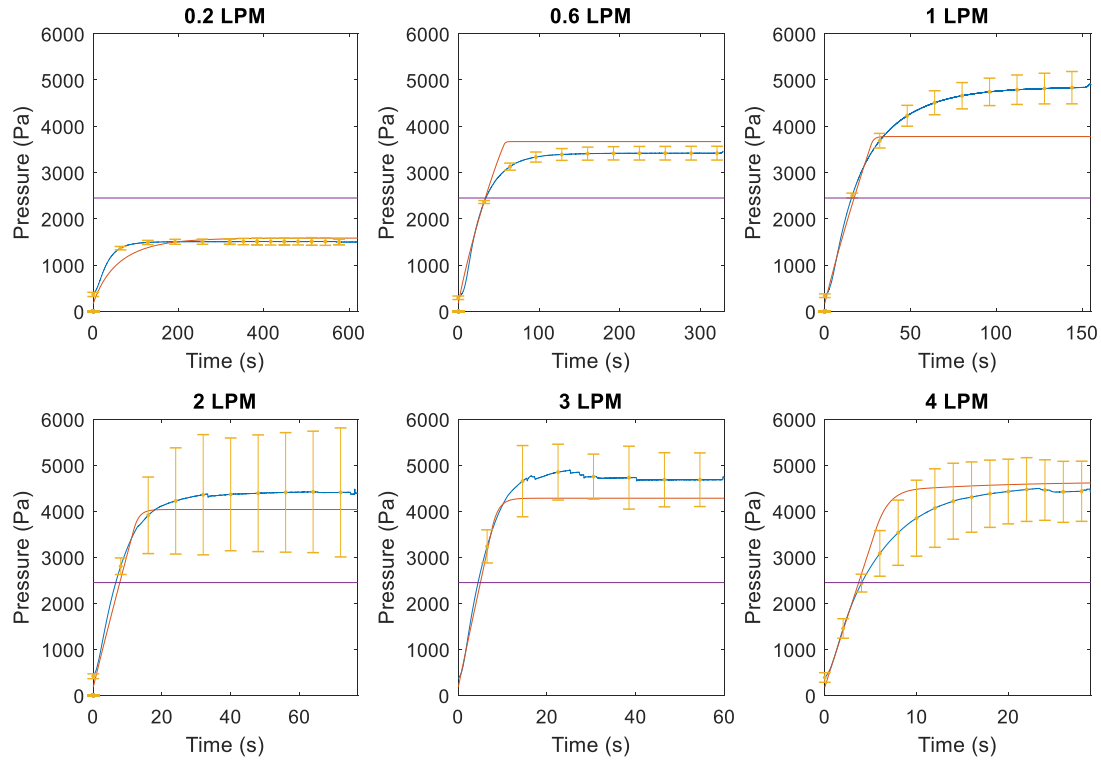


Figure 42. Experimental and Simulated Pressure Response of Pop-off Valve at 180 degrees at Various Flow Rates

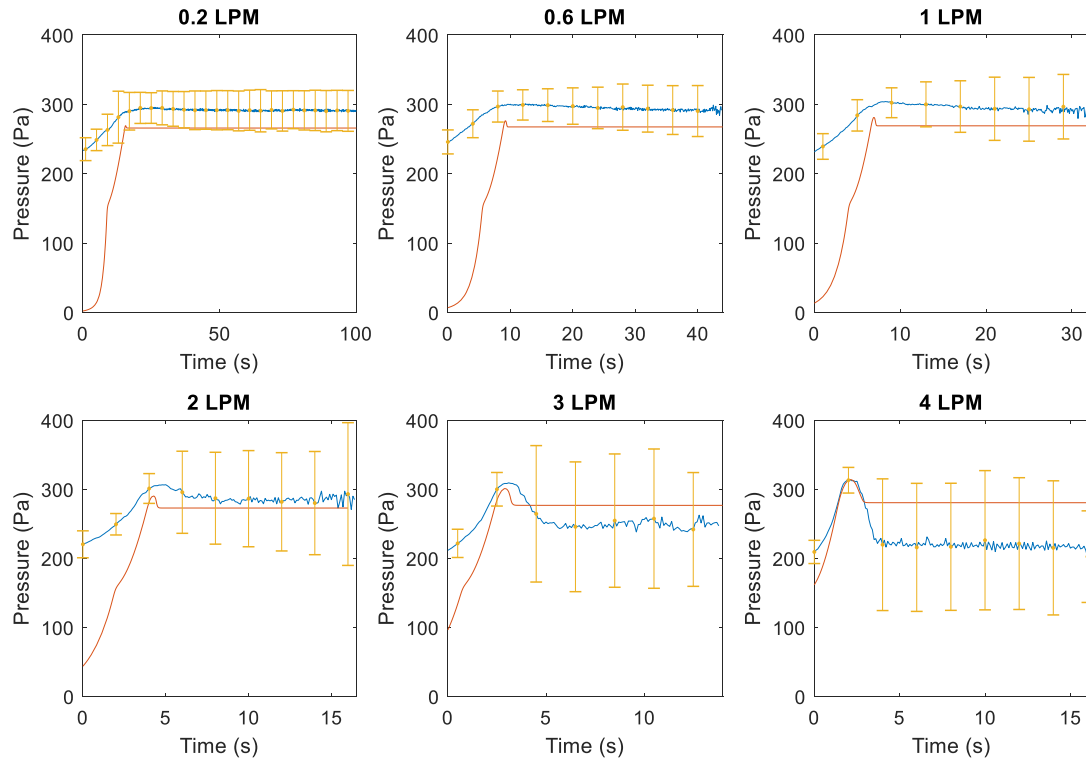


Figure 43. Experimental and Simulated Pressure Response of Pop-off Valve at 360 degrees at Various Flow Rates

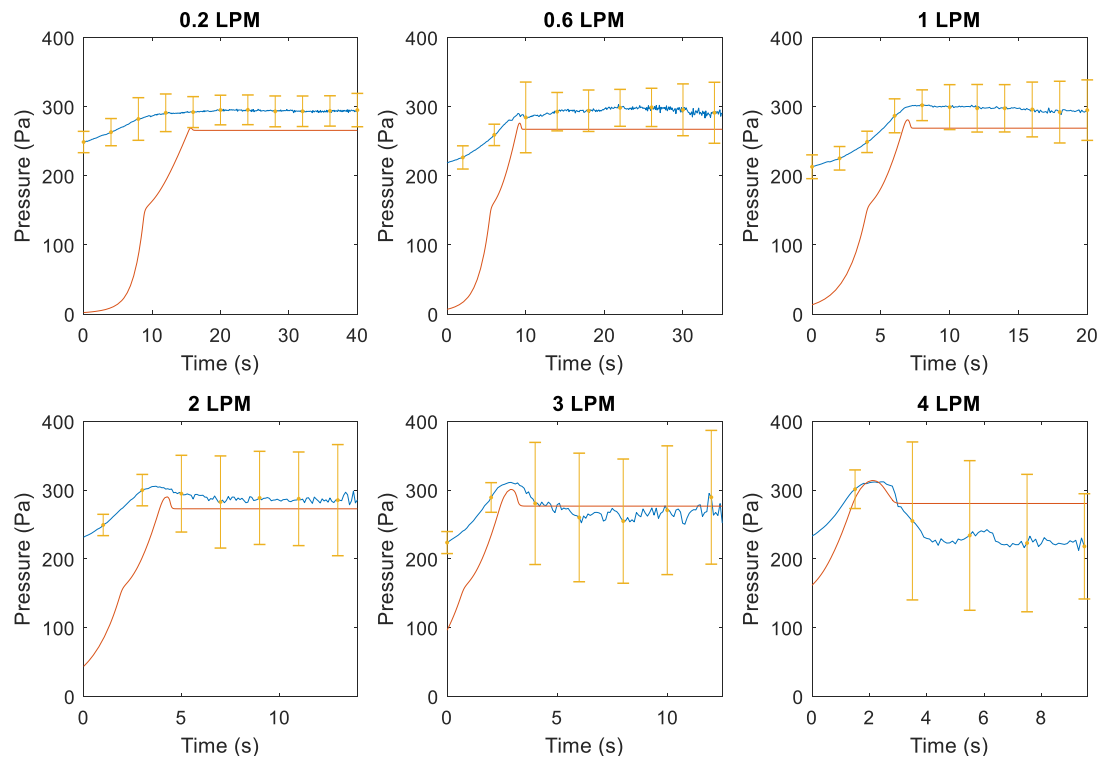


Figure 44. Experimental and Simulated Pressure Response of Pop-off Valve at 540 degrees at Various Flow Rates

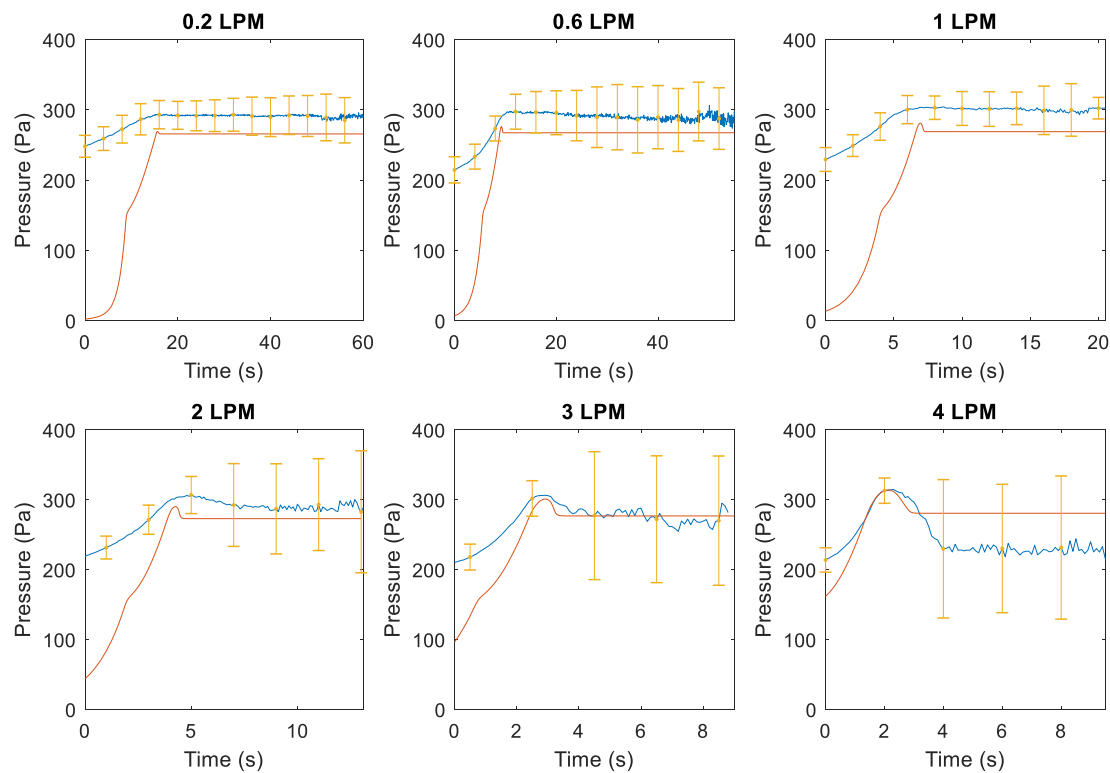


Figure 45. Experimental and Simulated Pressure Response of Pop-off Valve at 720 degrees at Various Flow Rates



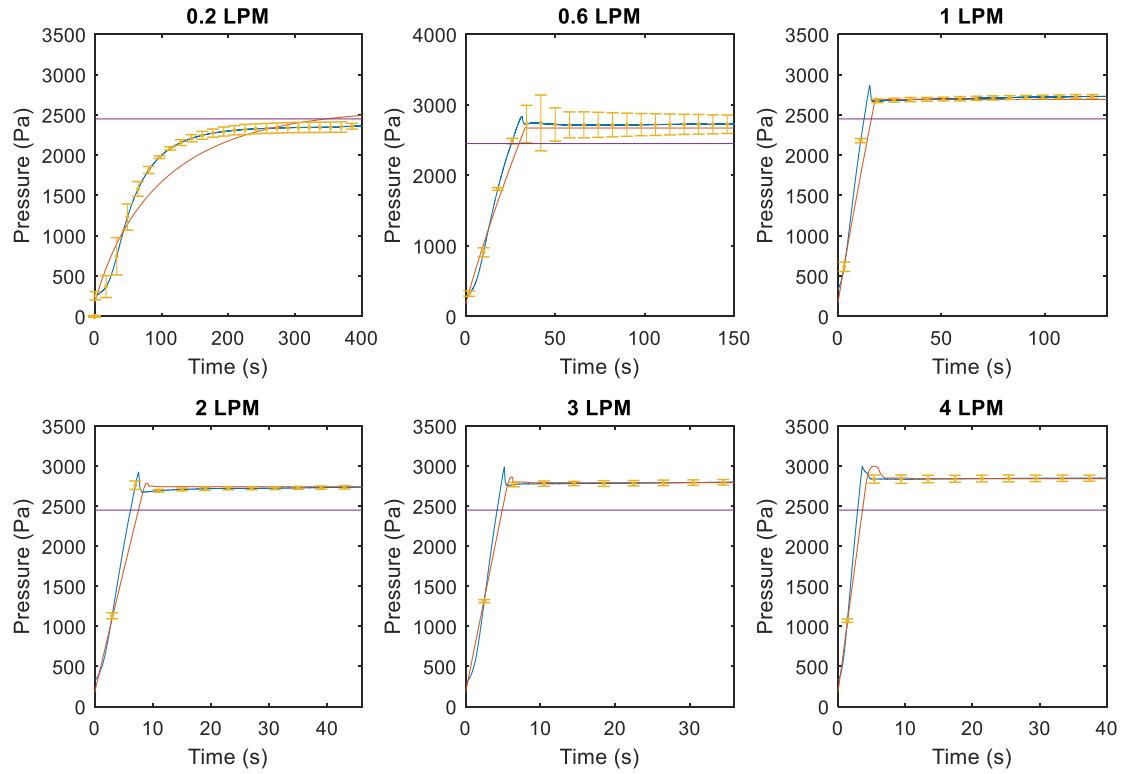


Figure 46. Experimental and Simulated Pressure Response of EMD Valve at Various Flow Rates

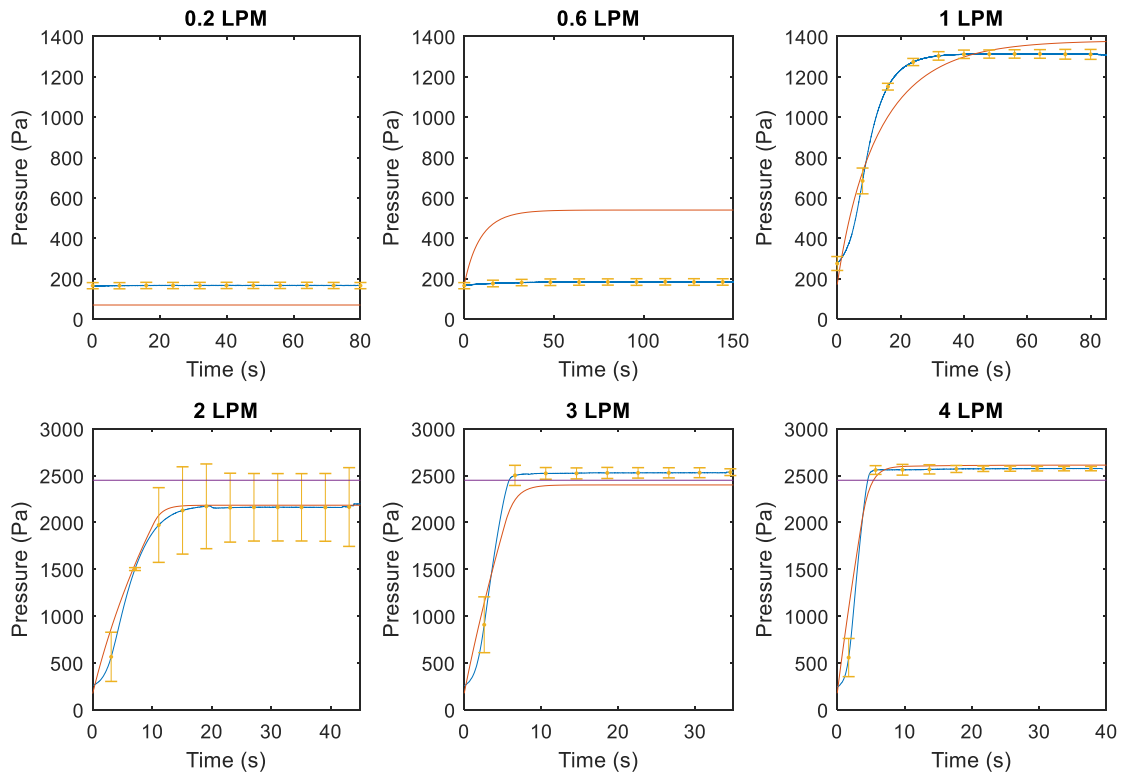


Figure 47. Experimental and Simulated Pressure Response of Reverse-PEEP Valve at Various Flow Rates

It is seen that the pop-off valve behaves almost identically for the openness values of 360, 540, and 720 degrees. For this reason, the behavior of the model for openness values of 540 and 720 degrees is not investigated. The shapes of the pressure response curves for these component blocks are well-matched to the components they represent. Table 5 shows the absolute and percent error of the steady state values of the component blocks relative to the experimental data.

The complete anesthesia system model was run for each of the six (6) test flow rates from 0.2 to 4 LPM for each of the three (3) pop-off Valve degrees of openness in three (3) configurations: with only the pop-off valve as pressure relief, with the EMD valve, and with the Reverse-PEEP valve. This was done both with a Patient Block and without. The plots in Figures 48-50 show the responses for the test flow rates without the patient block, and those in Figures 51-53 show the responses from the model with a patient block. Both figures show pressure in cmH<sub>2</sub>O to facilitate the comparison with the target relief pressure of 25 cm H<sub>2</sub>O.

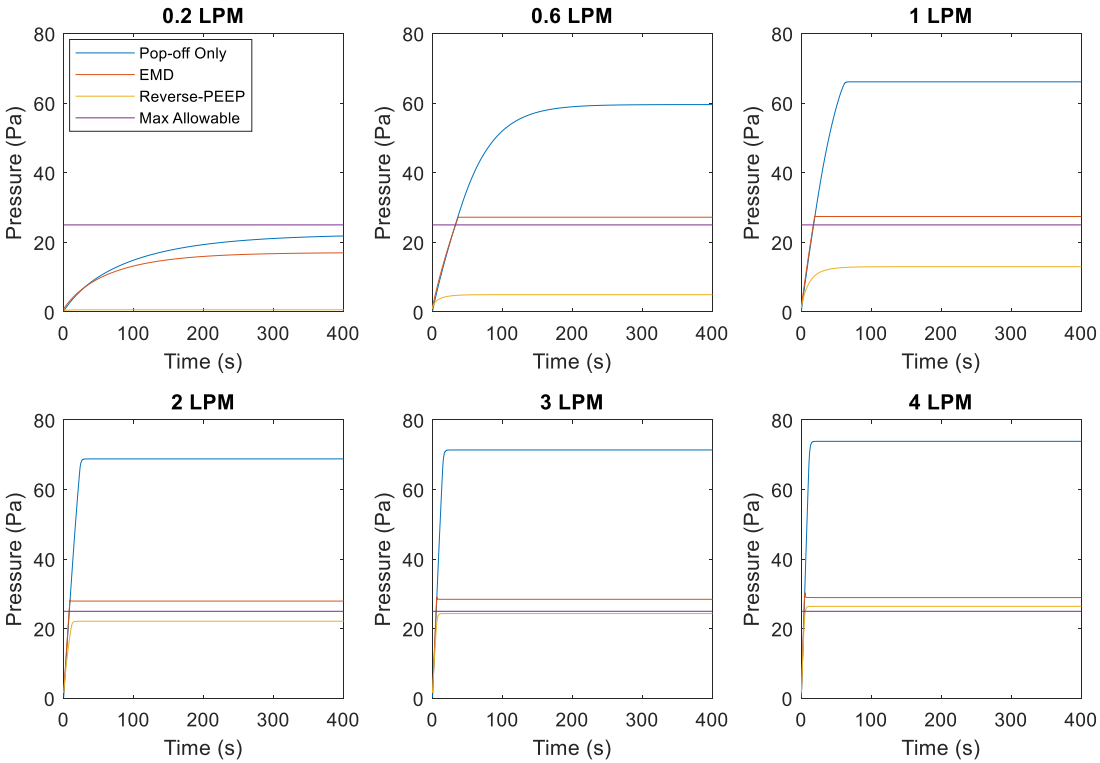


Figure 48. Pressure Response of Anesthesia System Model at Various Input Flow Rates, Pop-off Valve at 0 degrees

Table 5. Steady-state Error of Model Components

	Reservoir Bag	Pop-off Valve 0 degrees	Pop-off Valve 180 degrees	Pop-off Valve 360 degrees	Pop-off Valve 540 degrees	Pop-off Valve 720 degrees	EMD Valve	PEEP Valve
Flow Rate (LPM)	Abs. Error, Pa (Percent Error)	Abs. Error, Pa (Percent Error)	Abs. Error, Pa (Percent Error)	Abs. Error, Pa (Percent Error)	Abs. Error, Pa (Percent Error)	Abs. Error, Pa (Percent Error)	Abs. Error, Pa (Percent Error)	Abs. Error, Pa (Percent Error)
0.2	60 (1.8%)	300 (11.5%)	80 (5.3%)	20 (6.9%)	30 (10%)	20 (6.9%)	140 (5.9%)	90 (56.3%)
0.6	660 (9.3%)	500 (7.7%)	250 (7.3%)	20 (6.9%)	20 (6.9%)	20 (6.9%)	40 (1.5%)	360 (200%)
1	650 (9.1%)	550 (7.7%)	1060 (21.9%)	20 (6.9%)	20 (6.9%)	30 (10.%)	40 (1.5%)	60 (4.6%)
2	500 (6.9%)	450 (6.1%)	360 (8.2%)	20 (6.9%)	20 (6.9%)	20 (6.9%)	0 (0.0%)	20 (0.9%)
3	100 (1.4%)	120 (1.7%)	400 (8.5%)	30 (12%)	10 (3.6%)	10 (3.7%)	10 (0.4%)	140 (5.5%)
4	90 (1.2%)	50 (0.7%)	200 (4.5%)	60 (27%)	40 (14%)	50 (22%)	10 (0.4%)	30 (1.2%)

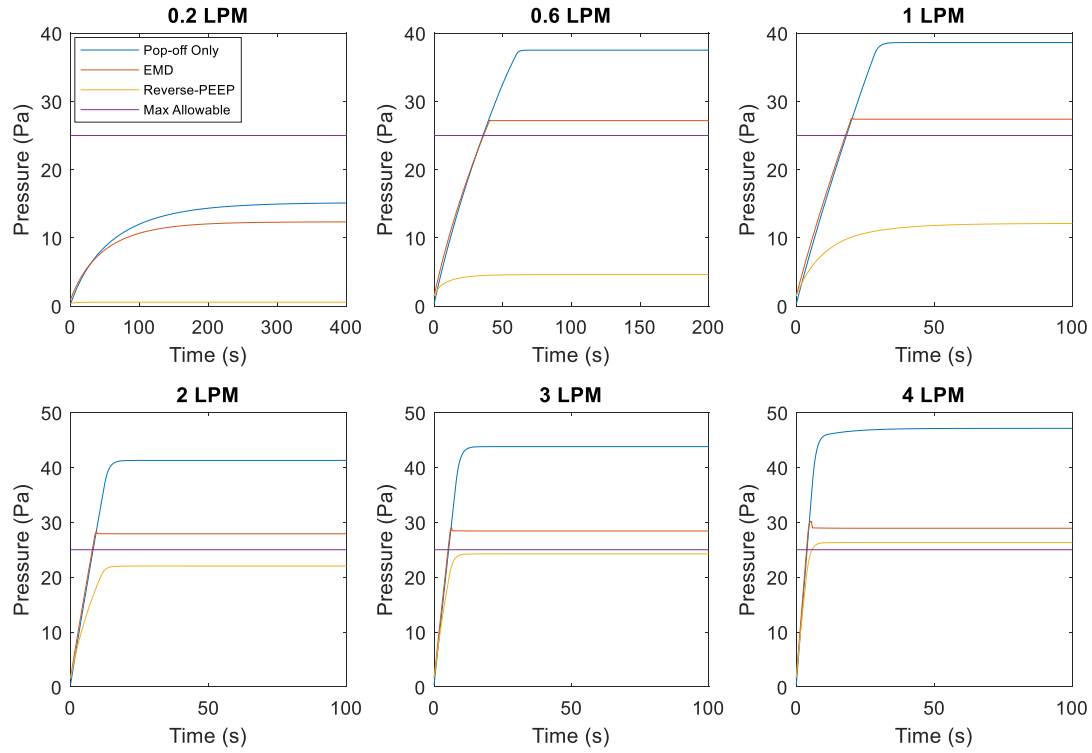


Figure 49. Pressure Response of Anesthesia System Model at Various Input Flow Rates, Pop-off Valve at 180 degrees

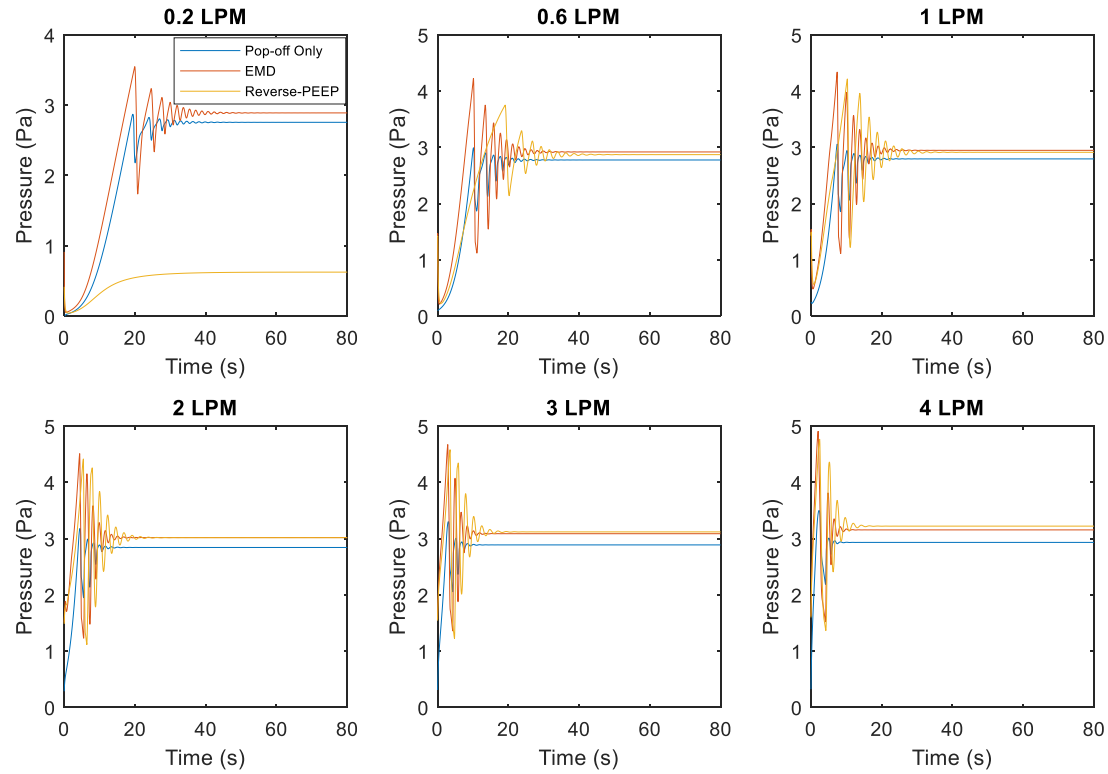


Figure 50. Pressure Response of Anesthesia System Model at Various Input Flow Rates, Pop-off Valve at 360 degrees

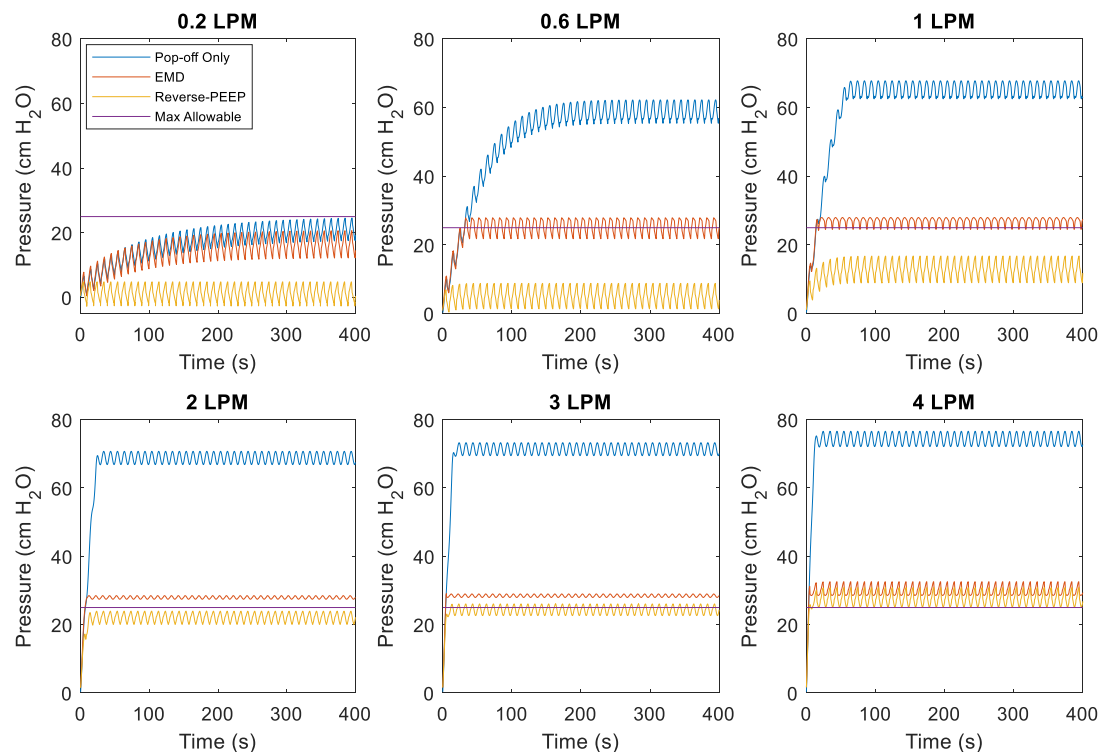


Figure 51. Pressure Response of Anesthesia System Model With Patient at Various Input Flow Rates, Pop-off Valve at 0 degrees

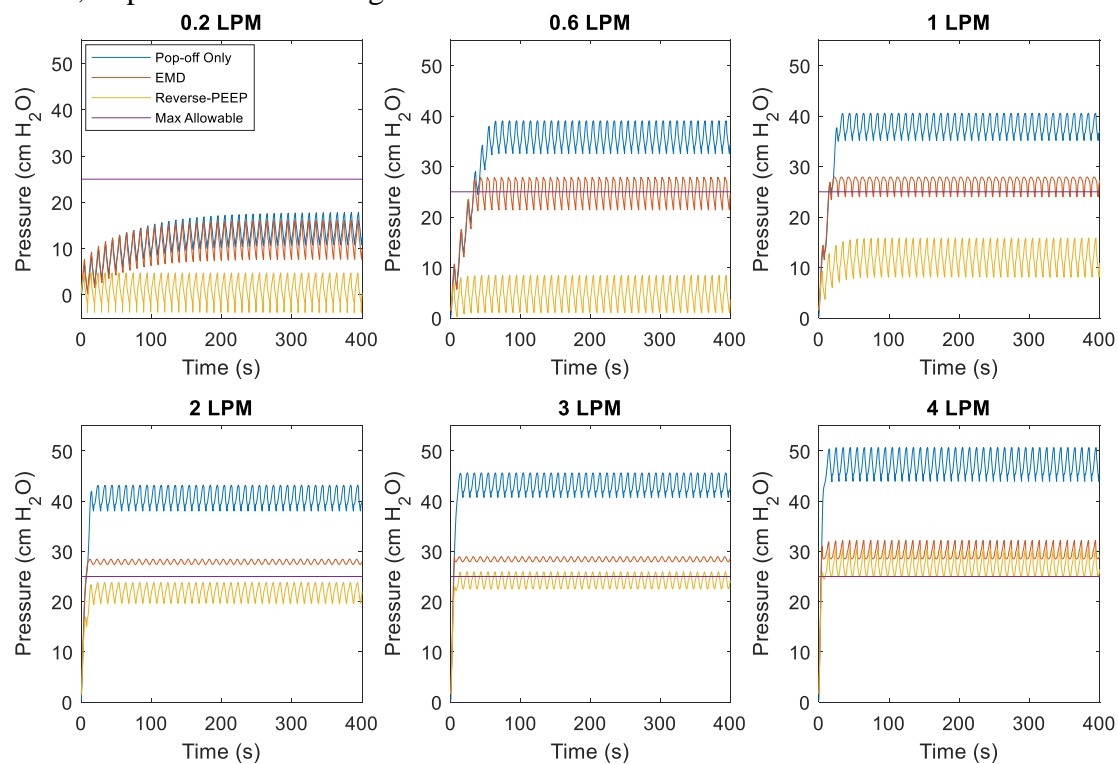


Figure 52. Pressure Response of Anesthesia System Model With Patient at Various Input Flow Rates, Pop-off Valve at 180 degrees

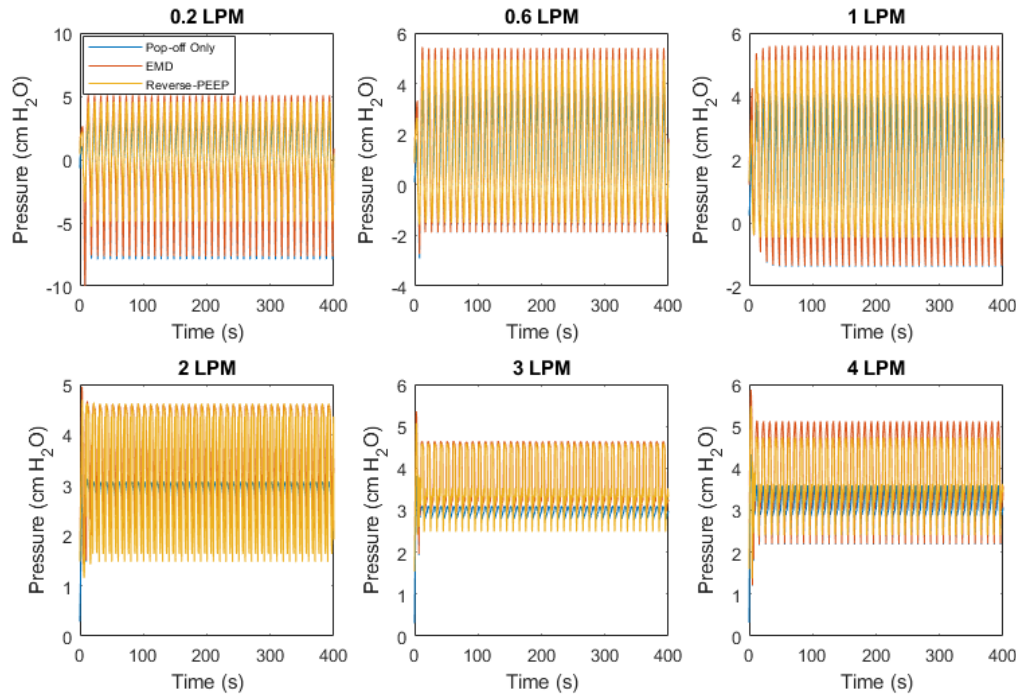


Figure 53. Pressure Response of Anesthesia System Model With Patient at Various Input Flow Rates, Pop-off Valve at 360 degrees

It can be easily seen that the EMD Valve consistently allows the pressure to reach higher values than the Reverse-PEEP configuration. It should also be noted that the addition of the patient block does not affect overall pressure response; it only causes the pressure of the system to oscillate.

The anesthesia system model was similarly run for 40 flow rates ranging from 0 to 4 LPM to obtain the plots seen in Figures 54-56. This was done excluding the patient block because the breathing flow rate varies from patient to patient. These plots of relief pressure vs. system flow rate summarize the behavior of the three configurations of the anesthesia system. Based on the convention of 30mL/min for each kilogram of weight of an animal, the EMD Valve allows the pressure to grow higher than the desired maximum of 25 cmH<sub>2</sub>O for animals weighing more than 9.50 kg [24]. The Reverse-PEEP Valve does not allow pressures higher than 25 cmH<sub>2</sub>O until a flow rate normal for animals weighing greater than 101 kg. Table 6 shows the flow rates causing a pressure of 25 cm H<sub>2</sub>O for both valves along with the corresponding patient weights. When the

pop-off valve is opened to 360 degrees, the pressure never reaches 25 cm H<sub>2</sub>O, so this configuration is excluded.

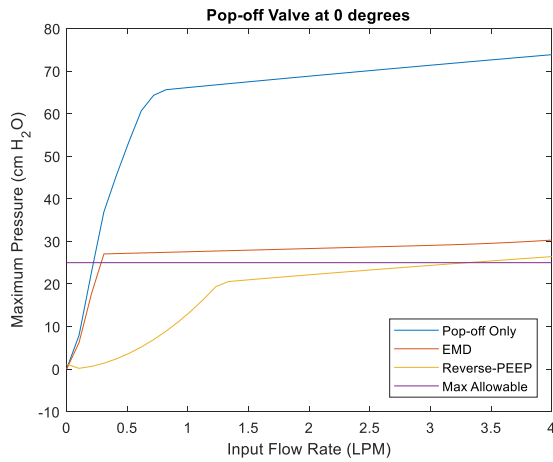


Figure 54. Maximum System Pressure, Pop-off Valve at 0 degrees

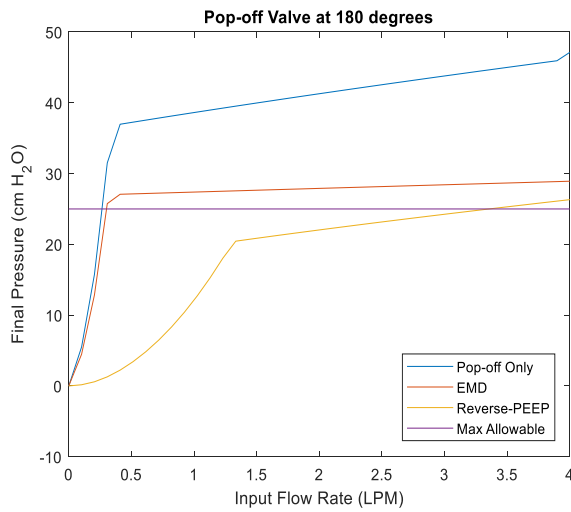


Figure 55. Maximum System Pressure, Pop-off Valve at 180 degrees

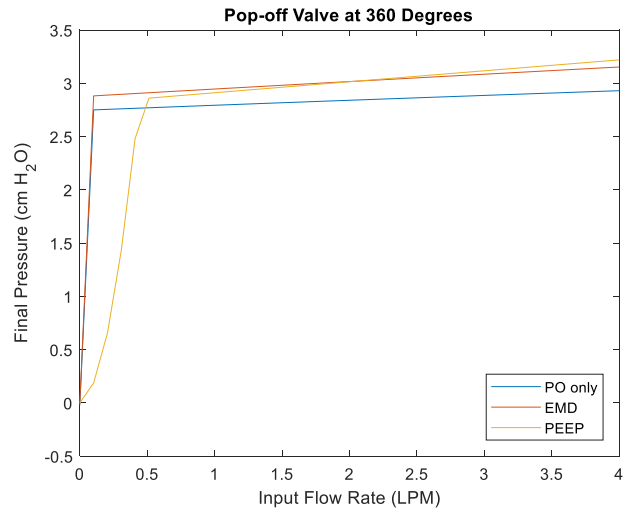


Figure 56. Maximum System Pressure, Pop-off Valve at 360 degrees

Table 6. Flow Rates and Corresponding Patient Weight at 25 cmH<sub>2</sub>O Maximum Pressure

	Pop-off at 0 degrees		Pop-off at 180 degrees	
	Flow Rate (LPM)	Weight (kg)	Flow Rate (LPM)	Weight (kg)
EMD	0.285	9.50	0.302	10.1
Reverse-PEEP	3.04	101	3.36	112

## Chapter 4. Conclusions

The results of this model are limited by the fact that only one of each component was used during data collection. It would be more desirable to collect data on multiple valves, as well as reservoir bags, carbon dioxide absorbers, and other circuit components, to ensure that the one measured was not an outlier. Additionally, the patient block in the model could be a more accurate representation of respiration. To improve this, the respiratory system model from Mešić et al [16] could be adapted for small animals instead of humans, and the resulting flow characteristic could be used instead of a sinusoidal flow source.

For the responses of the reservoir bag and various valves, the simulation gave a good approximation of the behavior of the real component. The shape and steady state pressure of the components were closely matched, with the average steady-state error being 12%. The model could be further improved by adding more pressure-measuring locations and comparing the full system simulation to the full anesthesia machine model, in addition to the isolated component comparisons. More accurate errors of pressure response could then be found, and the model could be adjusted accordingly.

Based on the results from the simulations, it can be concluded that the Reverse-PEEP valve configuration of the anesthesia machine is the most effective at keeping the system pressure below 25 cmH<sub>2</sub>O. However, it is noted that this configuration also leaks much of the anesthetic gas at low flow rates. This does not affect the effectiveness of the anesthesia machine for the patient, as the reservoir bag is still allowed to inflate at these low pressures. It does cause a hazardous environment for the veterinarians and other personnel in the operating room, as they could be inhaling the anesthetic agent. This risk is easily mitigated by adding an attachment to the PEEP valve, which sends the relieved gases to the scavenge system, containing the leakage.



A new valve design could be developed to address the needs of the anesthesia machine and eliminate the low-pressure leaking of the Reverse-PEEP valve. The existing Simscape model could be used to define the characteristics of a new valve, using the built-in relief valve block. Because this valve is parameterized by its opening area and other physical parameters, it could be used as a guide for valve design. A new valve should be compatible with anesthetic gases, reliable, and designed to fail-safe in the open position.

Based on the current available solutions and results of the model, veterinarians wishing to make their anesthesia machines safer for the patients should add the Reverse-PEEP Valve configuration with the scavenging system attachment to their anesthetic circuits.

## References

- [1] A. da Cunha, *LSU SVM Veterinary Anesthesia Class Notes*, 2016.
- [2] L. W. Hall, K. W. Clarke and C. M. Trim, *Veterinary Anaesthesia*, 10 ed., London: Harcourt Publishers Limited, 2001.
- [3] R. Stein, "Avoiding Pop-off Valve Related Fatalities," *Veterinary Anesthesia & Analgesia Support Group*, 24 March 2013. [Online]. Available: [http://www.vasg.org/avoiding\\_pop\\_off\\_valve\\_related\\_fatalities.htm](http://www.vasg.org/avoiding_pop_off_valve_related_fatalities.htm). [Accessed 8 September 2016].
- [4] B. O'Hagan and C. McKinnon, "A feline anaesthetic death associated with equipment incompatibility," *Australian Veterinary Journal*, vol. 91, no. 12, pp. 505-506, 2013.
- [5] M. Hellemans, *The Safety Relief Valve Handbook: Design and Use of Process Safety Valves to ASME and International Codes and Standards*, Elsevier, 2010.
- [6] B. K. Feller, "Anesthesia Complications - Code Blue!," *VetFolio*, 2015. [Online]. Available: <http://www.vetfolio.com/anesthesia/anesthesia-complications-code-blue>. [Accessed 15 September 2016].
- [7] D. R. M. McMurphy, D. D. S. Hodgson and B. M. P.H. Cribb, "Modification of a Nonrebreathing Circuit Adapter to Prevent Barotrauma in Anesthetized Patients," *Veterinary Anesthesia*, 1995.
- [8] R. Stein, "Reverse PEEP Positive Pressure Relief Valve," *Veterinary Anesthesia & Analgesia Support Group*, 3 March 2011. [Online]. Available: [http://www.vasg.org/reverse\\_peep\\_safety\\_valve.htm](http://www.vasg.org/reverse_peep_safety_valve.htm). [Accessed 2 October 2016].
- [9] "Pop-Off Occlusion Valve," *JD Medical Dist. Co., Inc*, 2008. [Online]. Available: <http://www.jdmedical.com/veterinary-products/anesthesia-accessories/pop-off-occlusion-valve/>. [Accessed September 18 2016].
- [10] "ACC311 Safety Pressure Relief Valve," *Supera Anesthesia Innovations*, 2014. [Online]. Available: <http://www.superavet.com/ACC311>. [Accessed 18 September 2016].
- [11] "EMD Safety Valve," *Essential Medical Devices, LLC*, 2016. [Online]. Available: <https://www.essentialmedicaldevices.com/>. [Accessed 21 September 2016].
- [12] R. A. Marrese and W. T. O'Sullivan, "Closed Exhaust Discharge System for Anesthesia Machines". Patent 3575196, 20 Apr. 1971.
- [13] R. Koehler and J. E. Donaldson, "Dual Valve, Anesthesia Machine Having Same, and Method for Using Same". U.S. Patent 5,743,257, 28 Oct 1996.

- [14] H. Latshaw, "Ventilation Valve for an Anesthesia System". U.S. Patent 8,925,547, 6 Jan. 2015.
- [15] J. G. C. Lerou and L. H. D. J. Booij, "Model-based administration of inhalation anaesthesia 1. Developing a system model," *British Journal of Anaesthesia*, vol. 86, no. 1, pp. 12-28, 2001.
- [16] S. Mešić, R. Babuška, H. C. Hoogsteden and A. F. M. Verbraak, "Computer-Controlled Mechanical Simulation of the Artificially Ventilated Human Respiratory System," *IEEE Transactions on Biomedical Engineering*, vol. 50, no. 6, pp. 731-743, 2003.
- [17] MathWorks, "MATLAB and Simulink in the World: Physical Modeling," 2016. [Online]. Available: <https://www.mathworks.com/company/newsletters/articles/matlab-and-simulink-in-the-world-physical-modeling.html>. [Accessed 17 July 2018].
- [18] MathWorks, "Simscape User's Guide," Natick, MA, 2018.
- [19] R. S. Figliola and D. E. Beasley, *Theory and Design for Mechanical Measurements*, John Wiley & Sons, Inc, 2011.
- [20] MathWorks, "Coefficient of Determination (R-Squared)," The MathWorks, Inc., 2018.
- [21] J. D. Anderson, *Modern Compressible Flow Third Edition*, New York, NY: McGraw-Hill, 2003.
- [22] H. Kreissl and R. Neiger, "Measurement of body temperature in 300 dogs with a novel noncontact infrared thermometer on the cornea in comparison to a standard rectal digital thermometer," *Journal of Veterinary Emergency and Critical Care*, vol. 25, no. 3, pp. 372-378, 2015.
- [23] A. Weil, "Overview of anesthetic machines and circuits (Proceedings)," CVC in San Diego Proceedings, San Diego, 2011.
- [24] W. W. Muir, J. A. E. Hubbell, R. Bednarski and P. Lerche, *Handbook of Veterinary Anesthesia*, 5 ed., St. Louis: Elsevier, 2013.
- [25] "VetTech," reddit.com, 14 January 2016. [Online]. Available: [https://www.reddit.com/r/VetTech/comments/40ypb4/an\\_unpleasant\\_anniversary/](https://www.reddit.com/r/VetTech/comments/40ypb4/an_unpleasant_anniversary/). [Accessed 2 October 2016].
- [26] K. Hunyady, "Anesthesia Cheat Sheet," [Online]. Available: [https://www.vetmed.wisc.edu/wp-content/uploads/2013/01/Anesthesia\\_Cheat\\_Sheet.pdf?y=15](https://www.vetmed.wisc.edu/wp-content/uploads/2013/01/Anesthesia_Cheat_Sheet.pdf?y=15). [Accessed 20 7 2017].
- [27] "DVM Solutions," [Online]. Available: <http://www.dvmsolutions.com/PCvetGard.htm>. [Accessed 17 07 2018].

## **Vita**

Corinne Duplantis, from Metairie, Louisiana, received her Bachelor's degree in mechanical engineering from Louisiana State University in May of 2017. During her undergraduate program, she participated in engineering internships in oil refining and manufacturing industries. She began the Accelerated Master's program during the final year of her Bachelor studies. Following completion of her Master's degree, she will assume a full-time engineering position in Baton Rouge.